

THEORY OF CIRCULAR DIELECTRIC WAVEGUIDE
WITH ANISOTROPIC SHEET COVER

BY

J.T. KISH
Department of Electrical Engineering
and Computer Science
University of Illinois at Chicago

Prepared under grant NAG2-544

**THEORY OF
CIRCULAR DIELECTRIC WAVEGUIDE
WITH ANISOTROPIC SHEET COVER**

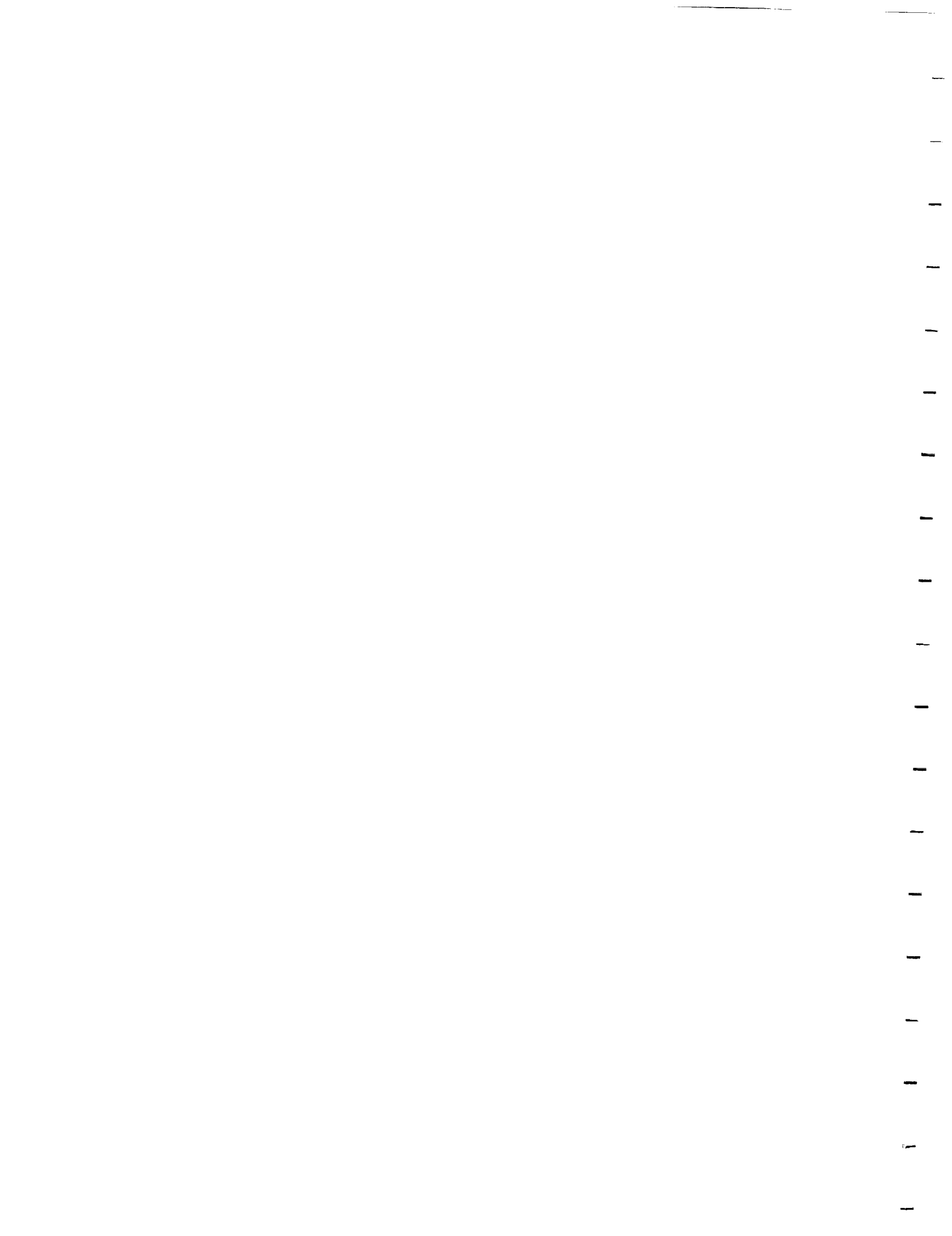
BY

JEROME THOMAS KISH
B.S., University of Illinois, Urbana, 1987

THESIS

Submitted as partial fulfillment of the requirements
for the degree of Master of Science in Electrical Engineering
in the Graduate College of the
University of Illinois at Chicago, 1990

Chicago, Illinois



ACKNOWLEDGEMENT

The author gratefully acknowledges the assistance of Professor P. L. E. Uslenghi of the University of Illinois at Chicago. This research was supported by the Pacific Missile Test Center and the NASA-Ames Research Center under grant NAG2-544. The author thanks John Kish for his illustrations.

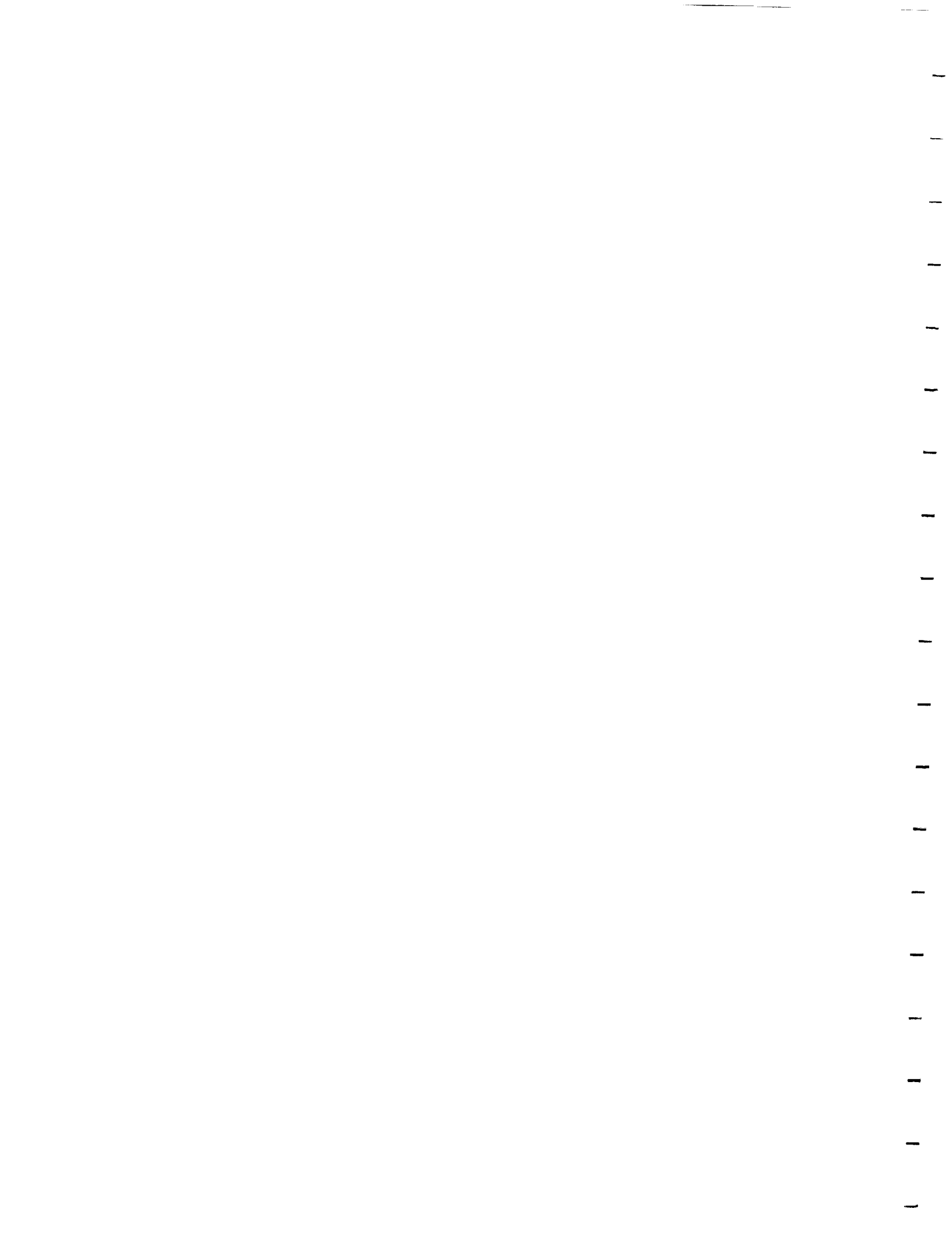


TABLE OF CONTENTS

<u>CHAPTER</u>	<u>PAGE</u>
1. INTRODUCTION	1
1.1 Background	1
1.2 Outline of Research	2
1.3 Geometry of Waveguide	3
2. FIELD SOLUTION	5
2.1 Field Components	5
2.2 Application of Boundary Conditions	7
2.3 Formulation of Dispersion Relation	8
2.4 Derivation of Cutoff Conditions	13
2.4.1 Limits at Cutoff	13
2.4.2 Case I. : $m > 1$	13
2.4.3 Case II. : $m = 1$	14
2.4.4 Case III. : $m = 0$	14
3. NUMERICAL RESULTS AND CONCLUSION	15
3.1 Lossless Sheet Parameters	15
3.2 Lossy Sheet Parameters	17
APPENDICES	29
Appendix A	29
Appendix B	34
CITED LITERATURE	37
VITA	38

LIST OF TABLES

<u>TABLE</u>	<u>PAGE</u>
I CUTOFF VALUES FOR LOSSLESS SHEETS	17

LIST OF FIGURES

<u>FIGURE</u>	<u>PAGE</u>
1 Waveguide cross section	3
2 Orientation of coordinate axis	3
3 Normalized propagation constant vs. normalized radius for step-index fiber	15
4 Normalized propagation constant vs. cutoff number, step-index fiber and circular, metallic guide	16
5 Normalized propagation constant vs. normalized radius for TM_{01} mode with real sheet admittances	18
6 Normalized attenuation constant vs. normalized radius for TM_{01} mode with real sheet admittances	19
7 Normalized propagation constant vs. normalized radius for TM_{01} mode with complex sheet admittances	20
8 Normalized attenuation constant vs. normalized radius for TM_{01} mode with complex sheet admittances	21
9 Normalized propagation constant vs. normalized radius for HE_{11} mode with real sheet admittances	22
10 Normalized attenuation constant vs. normalized radius for HE_{11} mode with real sheet admittances	23
11 Normalized propagation constant vs. normalized radius for HE_{11} mode with complex sheet admittances	24
12 Normalized attenuation constant vs. normalized radius for HE_{11} mode with complex sheet admittances	25
13 Normalized propagation constant vs. normalized radius for HE_{11} mode with complex sheet admittances and variation in parameter α	26
14 Normalized attenuation constant vs. normalized radius for HE_{11} mode with complex sheet admittances and variation in parameter α	27

SUMMARY

A circular dielectric waveguide consisting of an isotropic core covered with a thin anisotropic sheet is considered. The sheet is represented as a jump immittance and Maxwell's equations are applied. Solution of the boundary value problem yields the characteristic equation, or dispersion relation, which is then solved numerically. The results are verified for the step-index fiber and circular, metallic waveguides. Finally, examples are included to investigate the effects of the anisotropic sheet.

1. INTRODUCTION

1.1 Background

The solution to the problem of wave propagation in an isotropic, circularly symmetric optical waveguide is covered in many texts. In particular, each of references [1]-[3] provides an analysis of the step-index optical fiber. The step-index fiber is treated as a boundary-value problem which is solved by use of electromagnetic field theory and the separation of variables technique. The result is the characteristic equation of the guide and its solutions yield the propagation constants of the modes existing in the waveguide.

Recently, efforts have been made to find modal solutions for similar structures composed of anisotropic materials for applications in polarization maintaining optical fibers. Related structures composed of metallic waveguides coated with anisotropic layers have also been analyzed for radar cross section reduction purposes. In particular, Kapany and Burke [4] describe a circularly cylindrical waveguide with an isotropic cladding and an anisotropic core whose optical axis coincides with the axis of the cylinder. Tonning [5] reformulates the problem using a matrix formalism, and then extends the work of Kapany and Burke by examining a waveguide with a uniaxial core as well as cladding [6]. Another alternative approach is the variational analysis provided by Lindell and Oksanen [7] for the case of transverse anisotropy. Using this method, they compare their results to the exact eigenvalue equation for a metallic, circular guide coated with a layer characterized by an isotropic surface impedance [8]. For an anisotropic surface impedance, solutions have been obtained for propagation in the circular metallic guide [9]. Chou and Lee analyze the propagation and attenuation characteristics of a multilayered coated waveguide and then examine the radar cross section of the waveguide at near axial incidence [10]. Scattering from a multilayered cylindrical structure was studied by Graglia and Uslenghi [11] with each layer being represented by an anisotropic jump impedance. Thus there are a variety of methods available to analyze anisotropic structures.

1.1 Outline of Research

Using the jump immittance model, modal solutions will be obtained for a structure consisting of an isotropic, dielectric core covered with a thin anisotropic sheet surrounded by free space. The anisotropic sheet is modeled as a sheet of zero thickness with a jump admittance. The jump immittance model is convenient to implement and describes the electromagnetic behavior of a thin layer of penetrable material [12]. It is, therefore, possible to impose the appropriate boundary conditions and complete a field analysis using Maxwell's equations. The derivation follows that of the step-index optical fiber boundary value problem. The only difference is in the application of the boundary conditions as dictated by the jump immittance condition. The resulting dispersion relation, or eigenvalue equation, given in Section 2.3 describes the mode structure of the guide. Also derived are the cutoff conditions of the various modes (Section 2.4).

Since the jump admittance of the anisotropic sheet is generally complex in value, the dispersion relation and cutoff conditions are functions of complex variables. The solutions of these equations are the propagation and attenuation constants for the various modes that exist in the guide. As shown in Chapter 2, for limiting cases of the jump admittance, the dispersion relation and cutoff conditions approach the solutions for the isotropic step-index fiber and circular, metallic guide. To find the roots of complex-valued equations, the Newton-Raphson iterative procedure was employed [13]. The FORTRAN program constructed to apply the Newton-Raphson technique to the dispersion relation is given in Appendix A.

Chapter 3 provides the results of the numerical solution of the dispersion relation. First, the solutions are tested against known results for the step-index fiber and circular metallic guide. Next, cutoff values for the propagation constant are computed for the case of a lossless sheet. Finally, examples are included to illustrate how propagation and attenuation of the modes of the waveguide are affected by variations in the parameters of the anisotropic sheet.

1. **Introduction**
 2. **Background**
 3. **Methodology**
 4. **Results**
 5. **Discussion**
 6. **Conclusion**
 7. **References**
 8. **Appendix**
 9. **Figure 1**
 10. **Figure 2**
 11. **Figure 3**
 12. **Figure 4**
 13. **Figure 5**
 14. **Figure 6**
 15. **Figure 7**
 16. **Figure 8**
 17. **Figure 9**
 18. **Figure 10**
 19. **Figure 11**
 20. **Figure 12**
 21. **Figure 13**
 22. **Figure 14**
 23. **Figure 15**
 24. **Figure 16**
 25. **Figure 17**
 26. **Figure 18**
 27. **Figure 19**
 28. **Figure 20**
 29. **Figure 21**
 30. **Figure 22**
 31. **Figure 23**
 32. **Figure 24**
 33. **Figure 25**
 34. **Figure 26**
 35. **Figure 27**
 36. **Figure 28**
 37. **Figure 29**
 38. **Figure 30**
 39. **Figure 31**
 40. **Figure 32**
 41. **Figure 33**
 42. **Figure 34**
 43. **Figure 35**
 44. **Figure 36**
 45. **Figure 37**
 46. **Figure 38**
 47. **Figure 39**
 48. **Figure 40**
 49. **Figure 41**
 50. **Figure 42**
 51. **Figure 43**
 52. **Figure 44**
 53. **Figure 45**
 54. **Figure 46**
 55. **Figure 47**
 56. **Figure 48**
 57. **Figure 49**
 58. **Figure 50**
 59. **Figure 51**
 60. **Figure 52**
 61. **Figure 53**
 62. **Figure 54**
 63. **Figure 55**
 64. **Figure 56**
 65. **Figure 57**
 66. **Figure 58**
 67. **Figure 59**
 68. **Figure 60**
 69. **Figure 61**
 70. **Figure 62**
 71. **Figure 63**
 72. **Figure 64**
 73. **Figure 65**
 74. **Figure 66**
 75. **Figure 67**
 76. **Figure 68**
 77. **Figure 69**
 78. **Figure 70**
 79. **Figure 71**
 80. **Figure 72**
 81. **Figure 73**
 82. **Figure 74**
 83. **Figure 75**
 84. **Figure 76**
 85. **Figure 77**
 86. **Figure 78**
 87. **Figure 79**
 88. **Figure 80**
 89. **Figure 81**
 90. **Figure 82**
 91. **Figure 83**
 92. **Figure 84**
 93. **Figure 85**
 94. **Figure 86**
 95. **Figure 87**
 96. **Figure 88**
 97. **Figure 89**
 98. **Figure 90**
 99. **Figure 91**
 100. **Figure 92**
 101. **Figure 93**
 102. **Figure 94**
 103. **Figure 95**
 104. **Figure 96**
 105. **Figure 97**
 106. **Figure 98**
 107. **Figure 99**
 108. **Figure 100**
 109. **Figure 101**
 110. **Figure 102**
 111. **Figure 103**
 112. **Figure 104**
 113. **Figure 105**
 114. **Figure 106**
 115. **Figure 107**
 116. **Figure 108**
 117. **Figure 109**
 118. **Figure 110**
 119. **Figure 111**
 120. **Figure 112**
 121. **Figure 113**
 122. **Figure 114**
 123. **Figure 115**
 124. **Figure 116**
 125. **Figure 117**
 126. **Figure 118**
 127. **Figure 119**
 128. **Figure 120**
 129. **Figure 121**
 130. **Figure 122**
 131. **Figure 123**
 132. **Figure 124**
 133. **Figure 125**
 134. **Figure 126**
 135. **Figure 127**
 136. **Figure 128**
 137. **Figure 129**
 138. **Figure 130**
 139. **Figure 131**
 140. **Figure 132**
 141. **Figure 133**
 142. **Figure 134**
 143. **Figure 135**
 144. **Figure 136**
 145. **Figure 137**
 146. **Figure 138**
 147. **Figure 139**
 148. **Figure 140**
 149. **Figure 141**
 150. **Figure 142**
 151. **Figure 143**
 152. **Figure 144**
 153. **Figure 145**
 154. **Figure 146**
 155. **Figure 147**
 156. **Figure 148**
 157. **Figure 149**
 158. **Figure 150**
 159. **Figure 151**
 160. **Figure 152**
 161. **Figure 153**
 162. **Figure 154**
 163. **Figure 155**
 164. **Figure 156**
 165. **Figure 157**
 166. **Figure 158**
 167. **Figure 159**
 168. **Figure 160**
 169. **Figure 161**
 170. **Figure 162**
 171. **Figure 163**
 172. **Figure 164**
 173. **Figure 165**
 174. **Figure 166**
 175. **Figure 167**
 176. **Figure 168**
 177. **Figure 169**
 178. **Figure 170**
 179. **Figure 171**
 180. **Figure 172**
 181. **Figure 173**
 182. **Figure 174**
 183. **Figure 175**
 184. **Figure 176**
 185. **Figure 177**
 186. **Figure 178**
 187. **Figure 179**
 188. **Figure 180**
 189. **Figure 181**
 190. **Figure 182**
 191. **Figure 183**
 192. **Figure 184**
 193. **Figure 185**
 194. **Figure 186**
 195. **Figure 187**
 196. **Figure 188**
 197. **Figure 189**
 198. **Figure 190**
 199. **Figure 191**
 200. **Figure 192**
 201. **Figure 193**
 202. **Figure 194**
 203. **Figure 195**
 204. **Figure 196**
 205. **Figure 197**
 206. **Figure 198**
 207. **Figure 199**
 208. **Figure 200**
 209. **Figure 201**
 210. **Figure 202**
 211. **Figure 203**
 212. **Figure 204**
 213. **Figure 205**
 214. **Figure 206**
 215. **Figure 207**
 216. **Figure 208**
 217. **Figure 209**

1.3 Geometry of Waveguide

The cross section of the circularly symmetric waveguide is shown in Figure 1. A dielectric core of radius $\rho = a$ and index of refraction $n = \sqrt{\epsilon_r \mu_r}$ is coated by an anisotropic layer.

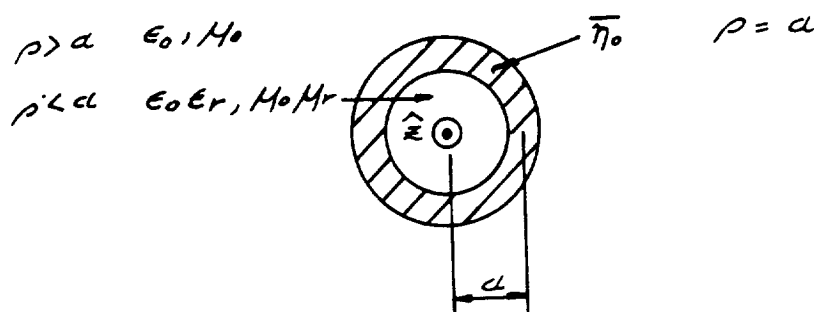


Figure 1. Waveguide cross section.

The layer is modeled with a jump admittance given by [11]:

$$(1) \quad \bar{\eta}_0 = Y_0 \begin{pmatrix} \eta_{01} & 0 \\ 0 & \eta_{02} \end{pmatrix}_{\zeta, \epsilon} ; \quad Y_0 = \sqrt{\epsilon_0 / \mu_0}$$

The coordinates of the sheet and rod are shown in Figure 2.

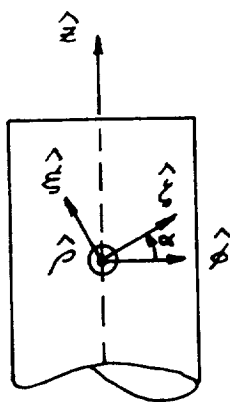
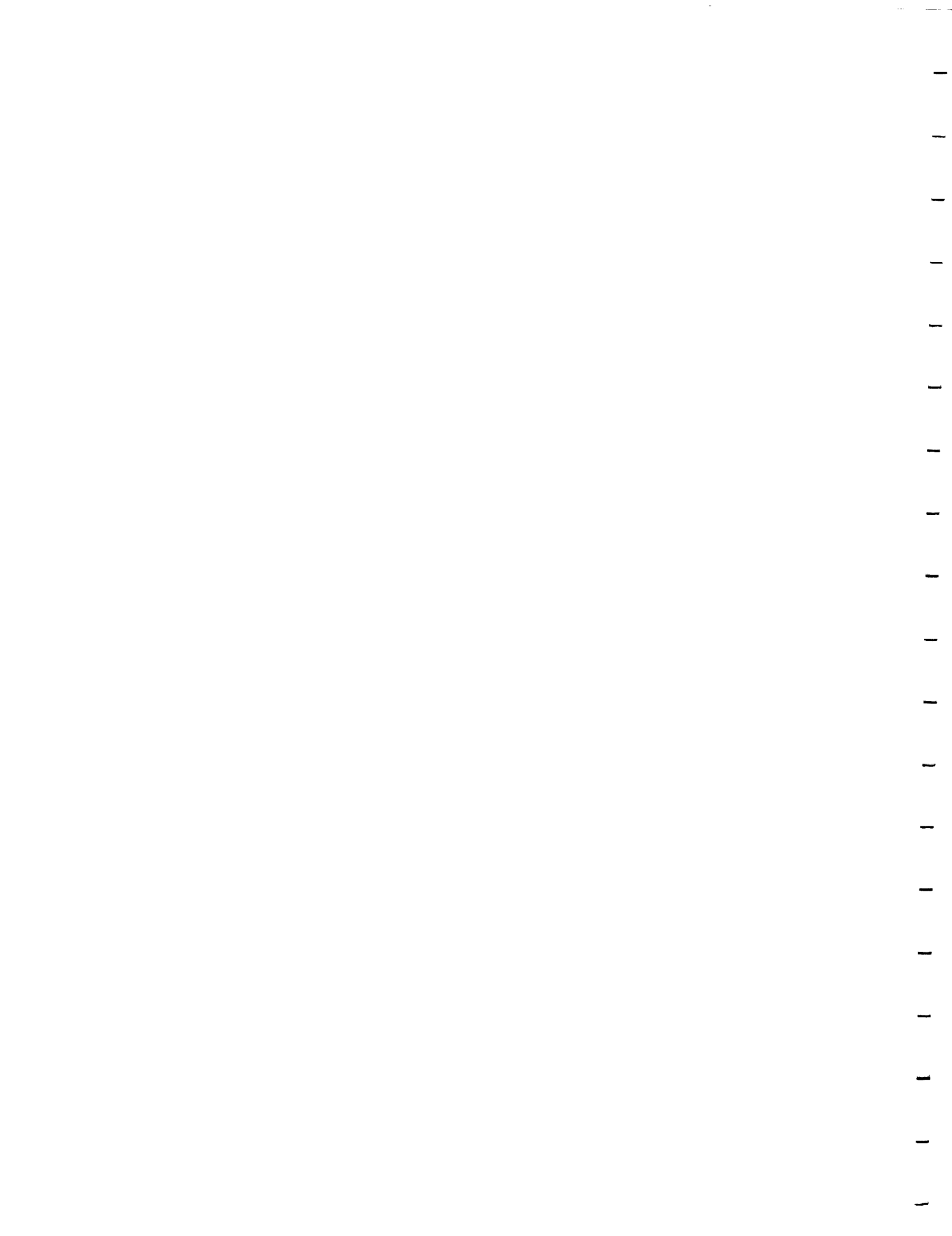


Figure 2. Orientation of coordinate axes.



A coordinate transformation [14] is performed represented by:

$$(2a) \quad \bar{\eta} = \mathbf{R} \bar{\eta}_0 \mathbf{R}^T,$$

where

$$(2b) \quad \mathbf{R} = \begin{pmatrix} \cos \alpha & -\sin \alpha \\ \sin \alpha & \cos \alpha \end{pmatrix}.$$

This transforms the arbitrary orientation of the sheet admittance into the ρ, ϕ, z coordinates of the rod. The result is:

$$(3) \quad \bar{\eta} = Y_0 \begin{pmatrix} \eta_1 & \eta_3 \\ \eta_3 & \eta_2 \end{pmatrix}_{\phi, z}$$

with

$$(4a) \quad \eta_1 = \eta_{01} \cos^2 \alpha + \eta_{02} \sin^2 \alpha$$

$$(4b) \quad \eta_2 = \eta_{01} \sin^2 \alpha + \eta_{02} \cos^2 \alpha$$

$$(4c) \quad \eta_3 = \sin \alpha \cos \alpha (\eta_{01} - \eta_{02})$$

2. FIELD SOLUTION

2.1 Field Components

Maxwell's curl equations for fields of angular frequency ω are, in the absence of sources:

$$(5a) \quad \nabla \times \mathbf{H} = j\omega\epsilon\mathbf{E}$$

$$(5b) \quad \nabla \times \mathbf{E} = -j\omega\mu\mathbf{H}.$$

We consider modes with longitudinal wave number β and attempt solutions of the form:

$$(6) \quad \mathbf{F} = \mathbf{F}(\rho)e^{-j\beta z + jm\phi + j\omega t}$$

where \mathbf{F} represents either the \mathbf{E} or \mathbf{H} field vector [6]. Note that

$$(7) \quad \frac{\partial \mathbf{F}}{\partial z} = -j\beta$$

Also, the periodicity of 2π radians in the variable ϕ requires that

$$(8) \quad \frac{\partial \mathbf{F}}{\partial \phi} = jm; \quad m = 0, \pm 1, \pm 2, \dots$$

The curls of (5) are expressed in the given cylindrical coordinates to produce a set of six scalar equations. With the use of (7) and (8), the transverse components E_ϕ, E_ρ, H_ϕ , and H_ρ may be expressed as functions of the longitudinal components E_z and H_z , as follows:

$$(9a) \quad E_\rho = \frac{1}{k_t^2} \left(-j\beta \frac{dE_z}{d\rho} + \frac{m\omega\mu}{\rho} H_z \right)$$

$$(9b) \quad E_\phi = \frac{1}{k_t^2} \left(\frac{m\beta}{\rho} E_z + j\omega\mu \frac{dH_z}{d\rho} \right)$$

$$(9c) \quad H_\rho = \frac{1}{k_t^2} \left(\frac{-m\omega\epsilon}{\rho} E_z - j\beta \frac{dH_z}{d\rho} \right)$$

$$(9d) \quad H_\phi = \frac{1}{k_t^2} \left(-j\omega\epsilon \frac{dE_z}{d\rho} + \frac{m\beta}{\rho} H_z \right).$$

The transverse wave number k_t is given by

$$(10a) \quad k_t^2 = k^2 - \beta^2$$

$$(10b) \quad k = \begin{cases} \omega \sqrt{\epsilon \mu} = k_0 n, & \rho < a \\ \omega \sqrt{\epsilon_0 \mu_0} = k_0, & \rho > a \end{cases}$$

For the region inside the core we must establish fields E_z and H_z which are finite at $\rho = 0$.

Choosing

$$(11) \quad k_t^2 = k_0^2 n^2 - \beta^2,$$

we have for $\rho < a$

$$(12) \quad F_z \propto J_m(k_t \rho) e^{jm\phi - j\beta z}.$$

Outside the core, an evanescent field is required, or

$$(13) \quad \begin{aligned} k_{0t}^2 &= k_0^2 - \beta^2 \\ &= -\gamma_t^2 < 0. \end{aligned}$$

We have for $\rho > a$

$$(14) \quad F_z \propto K_m(\gamma_t \rho) e^{jm\phi - j\beta z},$$

where K_m is the modified Bessel function of the second type. This guarantees exponential decay as $\rho \rightarrow \infty$. Also, both k_t^2 and γ_t^2 must be greater than zero for guidance. The bounds on β are then

$$(15) \quad k_0 n > \beta > k_0.$$

The resulting modal components of all fields are:

in the core, $\rho < a$:

$$(16a) \quad E_z = A J_m(k_t \rho) e^{jm\phi - j\beta z}$$

$$(16b) \quad H_z = B J_m(k_t \rho) e^{jm\phi - j\beta z}$$

$$(16c) \quad E_\rho = \left[\frac{-j\beta}{k_t} A J'_m(k_t \rho) + \frac{m\omega\mu}{k_t^2 \rho} B J_m(k_t \rho) \right] e^{jm\phi - j\beta z}$$

$$(16d) \quad E_\phi = \left[\frac{m\beta}{k_t^2 \rho} A J_m(k_t \rho) - \frac{j\beta}{k_t} B J'_m(k_t \rho) \right] e^{jm\phi - j\beta z}$$

$$(16e) \quad H_\rho = \left[\frac{-m\omega\epsilon}{k_t^2 \rho} A J_m(k_t \rho) - \frac{j\beta}{k_t} B J'_m(k_t \rho) \right] e^{jm\phi - j\beta z}$$

$$(16f) \quad H_\phi = \left[\frac{-j\omega\epsilon}{k_t} A J'_m(k_t \rho) + \frac{m\beta}{k_t^2 \rho} B J_m(k_t \rho) \right] e^{jm\phi - j\beta z},$$

and outside the core, $\rho > a$:

$$(17a) \quad E_z = C K_m(\gamma_t \rho) e^{jm\phi - j\beta z}$$

$$(17b) \quad H_z = D K_m(\gamma_t \rho) e^{jm\phi - j\beta z}$$

$$(17c) \quad E_\rho = \left[\frac{-\beta}{j\gamma_t} C K'_m(\gamma_t \rho) - \frac{m\omega\mu_0}{\gamma_t^2 \rho} D K_m(\gamma_t \rho) \right] e^{jm\phi - j\beta z}$$

$$(17d) \quad E_\phi = \left[-\frac{m\beta}{\gamma_t^2 \rho} C K_m(\gamma_t \rho) + \frac{\omega\mu_0}{j\gamma_t} D K'_m(\gamma_t \rho) \right] e^{jm\phi - j\beta z}$$

$$(17e) \quad H_\rho = \left[\frac{m\omega\epsilon_0}{\gamma_t^2 \rho} C K_m(\gamma_t \rho) - \frac{\beta}{j\gamma_t} D K'_m(\gamma_t \rho) \right] e^{jm\phi - j\beta z}$$

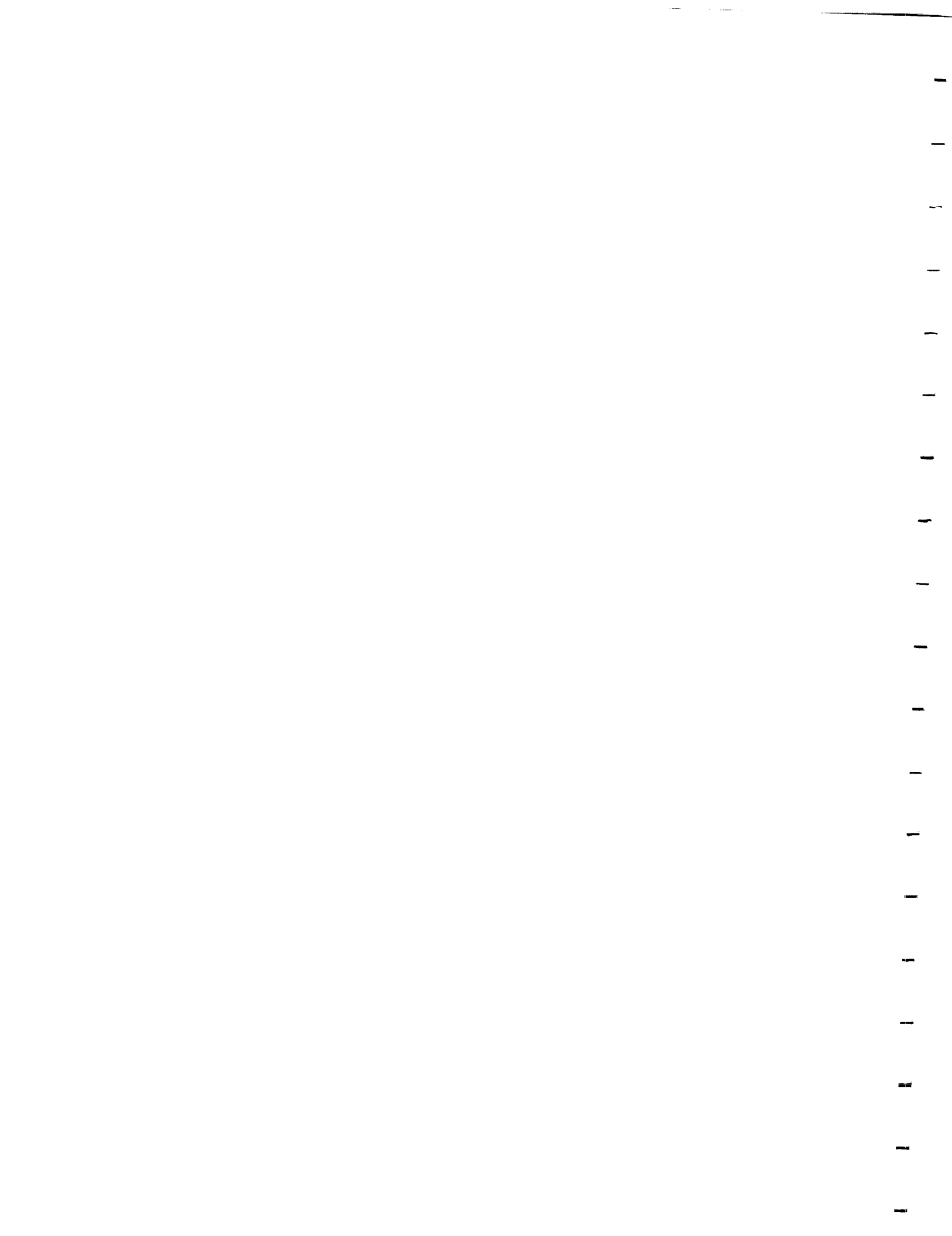
$$(17f) \quad H_\phi = \left[-\frac{\omega\epsilon_0}{j\gamma_t} C K'_m(\gamma_t \rho) - \frac{m\beta}{\gamma_t^2 \rho} D K_m(\gamma_t \rho) \right] e^{jm\phi - j\beta z}.$$

2.2 Application of Boundary Conditions

We have already satisfied the boundary conditions at $\rho = 0$ and as $\rho \rightarrow \infty$ as described by (12) and (14). Across the interface at $\rho = a$, the tangential electric field is continuous:

$$(18a) \quad (E_z)_{\rho=a-} = (E_z)_{\rho=a+}$$

$$(18b) \quad (E_\phi)_{\rho=a-} = (E_\phi)_{\rho=a+}.$$



The tangential magnetic field is discontinuous and satisfies the jump condition [10]:

$$(19) \quad \hat{\rho} \times (\mathbf{H}_{\rho=a_+} - \mathbf{H}_{\rho=a_+-}) = \bar{\eta}(\mathbf{E}_{\text{tan}})_{\rho=a} ,$$

or,

$$(20a) \quad -H_z(a_+) + H_z(a_-) = Y_0[\eta_1 E_\phi(a) + \eta_3 E_z(a)]$$

$$(20b) \quad H_\phi(a_+) - H_\phi(a_-) = Y_0[\eta_3 E_\phi(a) + \eta_2 E_z(a)].$$

Equations (18) and (20) will be applied to the field equations of (16) and (17). The result is a homogeneous system of four equations in the four unknowns $A, B, C,$ and D ,

$$(21) \quad \mathbf{M} \begin{pmatrix} A \\ B \\ C \\ D \end{pmatrix} = 0.$$

For a nontrivial solution it is necessary that $\det \mathbf{M} = 0$. The resulting equation is known as the dispersion relation.

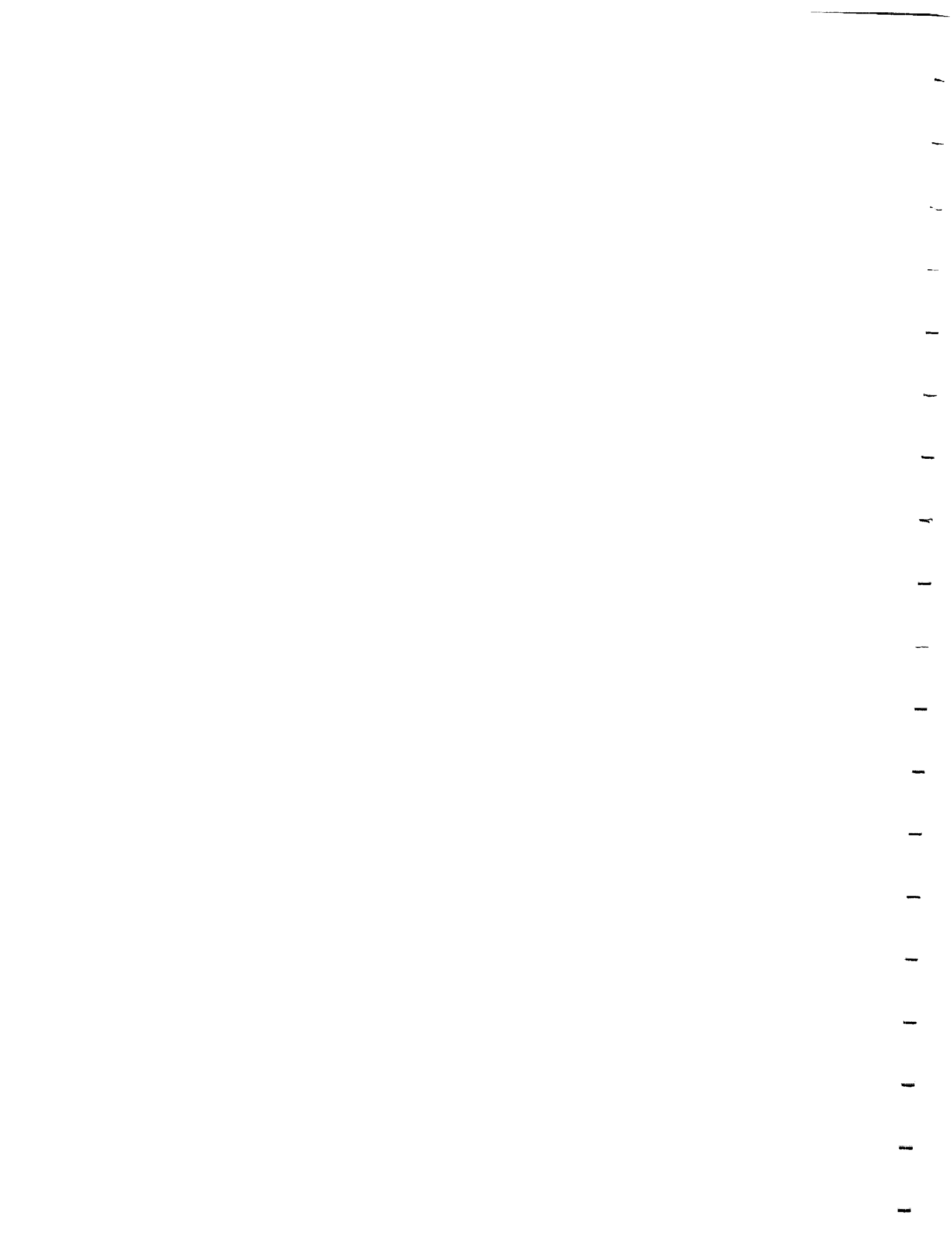
2.3 Formulation of Dispersion Relation

As shown in (21), the coefficients $A, B, C,$ and $D,$ are chosen as the column vector and (18) and (20) are the rows. The right hand sides of (20) are evaluated at $\rho = a_-$. The matrix \mathbf{M} becomes:

$$(22) \quad \mathbf{M} = \begin{pmatrix} J_m(k_t a) & 0 & -K_m(\gamma_t a) & 0 \\ \frac{m\beta}{k_t^2 a} J_m(k_t a) & \frac{j\omega\mu}{k_t} J'_m(k_t a) & \frac{m\beta}{\gamma_t^2 a} K_m(\gamma_t a) & \frac{-\omega\mu_0}{j\gamma_t} K'_m(\gamma_t a) \\ -Y_0 J_m(k_t a)(\eta_3 + \eta_1 \frac{m\beta}{k_t^2 a}) & J_m(k_t a) & 0 & -K_m(\gamma_t a) \\ \frac{-j\omega\epsilon}{k_t} J'_m(k_t a) & \frac{m\beta}{k_t^2 a} J_m(k_t a) & \frac{\omega\epsilon_0}{j\gamma_t} K'_m(\gamma_t a) & \frac{m\beta}{\gamma_t^2 a} K_m(\gamma_t a) \\ + Y_0(\eta_2 + \eta_3 \frac{m\beta}{k_t^2 a}) J_m(k_t a) & + Y_0 \eta_3 \frac{j\omega\mu}{k_t} J'_m(k_t a) & & \end{pmatrix}$$

Taking the determinant of (22):

$$(23) \quad \begin{vmatrix} \frac{j\omega\mu}{k_t} J'_m(k_t a) & \frac{m\beta}{\gamma_t^2 a} K_m(\gamma_t a) & -\frac{\omega\mu_0}{j\gamma_t} K'_m(\gamma_t a) \\ J_m(k_t a) - Y_0 \eta_1 \frac{j\omega\mu}{k_t} J'_m(k_t a) & 0 & -K_m(\gamma_t a) \\ \frac{m\beta}{k_t^2 a} J_m(k_t a) + Y_0 \eta_3 \frac{j\omega\mu}{k_t} J'_m(k_t a) & \frac{\omega\epsilon_0}{j\gamma_t} K'_m(\gamma_t a) & \frac{m\beta}{\gamma_t^2 a} K_m(\gamma_t a) \end{vmatrix} \\ - K_m(\gamma_t a) \begin{vmatrix} \frac{m\beta}{k_t^2 a} J_m(k_t a) & \frac{j\omega\mu}{k_t} J'_m(k_t a) & \frac{-\omega\mu_0}{j\gamma_t} K'_m(\gamma_t a) \\ -Y_0 J_m(k_t a)(\eta_3 + \eta_1 \frac{m\beta}{k_t^2 a}) & J_m(k_t a) & -K_m(\gamma_t a) \\ \frac{-j\omega\epsilon}{k_t} J'_m(k_t a) & \frac{m\beta}{k_t^2 a} J_m(k_t a) & \frac{m\beta}{\gamma_t^2 a} K_m(\gamma_t a) \\ + Y_0(\eta_2 + \eta_3 \frac{m\beta}{k_t^2 a}) J_m(k_t a) & + Y_0 \eta_3 \frac{j\omega\mu}{k_t} J'_m(k_t a) & \end{vmatrix} = 0.$$



This last expression leads to the following result:

$$\begin{aligned}
 & \frac{n^2 k_0^2}{k_t^2} \left(\frac{J'_m(k_t a)}{k_t J_m(k_t a)} \right)^2 + \frac{j k_0^2}{k_t \gamma_t} \frac{J'_m(k_t a)}{k_t J_m(k_t a)} \frac{K'_m(\gamma_t a)}{j \gamma_t K_m(\gamma_t a)} (\epsilon/\epsilon_0 + \mu/\mu_0) \\
 & - \frac{k_0^2}{\gamma_t^2} \left(\frac{K'_m(\gamma_t a)}{j \gamma_t K_m(\gamma_t a)} \right)^2 - \left(\frac{m\beta}{a} \right)^2 \left(\frac{1}{\gamma_t^2} + \frac{1}{k_t^2} \right)^2 \\
 & + \frac{j \omega^2 \mu^2 \mu_r}{k_t \gamma_t} Y_0^2 \frac{J'_m(k_t a)}{k_t J_m(k_t a)} \frac{K'_m(\gamma_t a)}{j \gamma_t K_m(\gamma_t a)} (\eta_1 \eta_2 - \eta_3^2) \\
 & + \frac{\omega}{\gamma_t k_t} Y_0 \eta_1 \frac{J'_m(k_t a)}{k_t J_m(k_t a)} \frac{K'_m(\gamma_t a)}{j \gamma_t K_m(\gamma_t a)} \left(\frac{\mu_0 n^2 k_0^2}{k_t} \frac{J'_m(k_t a)}{k_t J_m(k_t a)} + \frac{j \mu k_0^2}{\gamma_t} \frac{K'_m(\gamma_t a)}{j \gamma_t K_m(\gamma_t a)} \right) \\
 & + \frac{j \omega \mu}{k_t} Y_0 \frac{J'_m(k_t a)}{k_t J_m(k_t a)} \left[\left(\frac{m\beta_0}{\gamma_t^2 a} \right)^2 \eta_1 - 2 \frac{m\beta_0}{\gamma_t^2 a} \eta_3 + \eta_2 \right] \\
 & - \frac{\omega \mu_0}{\gamma_t} Y_0 \frac{K'_m(\gamma_t a)}{j \gamma_t K_m(\gamma_t a)} \left[\left(\frac{m\beta_0}{k_t^2 a} \right)^2 \eta_1 + 2 \frac{m\beta_0}{k_t^2 a} \eta_3 + \eta_2 \right] = 0.
 \end{aligned}
 \tag{24}$$

To develop a general case, normalized variables [4] are introduced according to the following equations:

$$(25a) \quad b_0 = \beta/k_0$$

$$(25b) \quad k_{t0} = k_t/k_0$$

$$(25c) \quad \gamma_{t0} = \gamma_t/k_0$$

$$(25d) \quad a_0 = a k_0.$$

The guidance condition becomes:

$$(26) \quad n > b_0 > 1.$$

Equation (24) becomes:

$$\begin{aligned}
 (27) \quad & \epsilon_r \mu_r \left(\frac{J'_m(k_{t0}a_0)}{k_{t0}J_m(k_{t0}a_0)} \right)^2 + \frac{J'_m(k_{t0}a_0)}{k_{t0}J_m(k_{t0}a_0)} \frac{K'_m(\gamma_{t0}a_0)}{\gamma_{t0}K_m(\gamma_{t0}a_0)} (\epsilon_r + \mu_r) \\
 & + \left(\frac{K'_m(\gamma_{t0}a_0)}{\gamma_{t0}K_m(\gamma_{t0}a_0)} \right)^2 - \left(\frac{mb_0}{a_0} \right)^2 \left(\frac{1}{\gamma_{t0}^2} + \frac{1}{k_{t0}^2} \right)^2 \\
 & + \mu_r \frac{J'_m(k_{t0}a_0)}{k_{t0}J_m(k_{t0}a_0)} \frac{K'_m(\gamma_{t0}a_0)}{\gamma_{t0}K_m(\gamma_{t0}a_0)} (\eta_1 \eta_2 - \eta_3^2) \\
 & - j \eta_1 \mu_r \frac{J'_m(k_{t0}a_0)}{k_{t0}J_m(k_{t0}a_0)} \frac{K'_m(\gamma_{t0}a_0)}{\gamma_{t0}K_m(\gamma_{t0}a_0)} \left(\epsilon_r \frac{J'_m(k_{t0}a_0)}{k_{t0}J_m(k_{t0}a_0)} + \frac{K'_m(\gamma_{t0}a_0)}{\gamma_{t0}K_m(\gamma_{t0}a_0)} \right) \\
 & + j \mu_r \frac{J'_m(k_{t0}a_0)}{k_{t0}J_m(k_{t0}a_0)} \left[\left(\frac{mb_0}{\gamma_{t0}^2 a_0} \right)^2 \eta_1 - 2 \frac{mb_0}{\gamma_{t0}^2 a_0} \eta_3 + \eta_2 \right] \\
 & + j \frac{K'_m(\gamma_{t0}a_0)}{\gamma_{t0}K_m(\gamma_{t0}a_0)} \left[\left(\frac{mb_0}{k_{t0}^2 a_0} \right)^2 \eta_1 + 2 \frac{mb_0}{k_{t0}^2 a_0} \eta_3 + \eta_2 \right] = 0.
 \end{aligned}$$

To write more compactly, let

$$(28a) \quad u = k_{t0}a_0$$

$$(28b) \quad q = \gamma_{t0}a_0$$

$$(28c) \quad \mathcal{J}_m = \frac{J'_m(u)}{uJ_m(u)}$$

$$(28d) \quad \mathcal{K}_m = \frac{K'_m(q)}{qK_m(q)}$$

Note that the dispersion relation is quadratic in \mathcal{J}_m . It is of the form

$$(29) \quad C_0 \mathcal{J}_m^2 + C_1 \mathcal{J}_m + C_2 = 0 \quad .$$

Collecting terms,

$$\begin{aligned}
 & \mathcal{J}_m^2 \epsilon_r \mu_r (1 - j \eta_1 a_0 \mathcal{K}_m) \\
 & + \mathcal{J}_m \left\{ -j \eta_1 \mu_r a_0 \mathcal{K}_m^2 + \mathcal{K}_m [\mu_r (1 + \eta_1 \eta_2 - \eta_3^2) + \epsilon_r] \right. \\
 & \quad \left. + \frac{j \mu_r}{a_0} \left[\left(\frac{mb_0 a_0}{q^2} \right)^2 \eta_1 - 2 \frac{mb_0 a_0}{q^2} \eta_3 + \eta_2 \right] \right\} \\
 (30) \quad & + \mathcal{K}_m^2 + \frac{j \mathcal{K}_m}{a_0} \left[\left(\frac{mb_0 a_0}{u^2} \right)^2 \eta_1 + 2 \frac{mb_0 a_0}{u^2} \eta_3 + \eta_2 \right] - (mb_0)^2 \left(\frac{1}{u^2} + \frac{1}{q^2} \right)^2 = 0 .
 \end{aligned}$$

The step-index solution is contained in the real portion of (30), while the anisotropic sheet adds additional complex terms. In this form, the dispersion relation is solved numerically; its roots are computed as explained in Appendix A. The solutions are [4]:

$$(31a) \quad \text{EH}_{mn} \text{ modes : } \mathcal{J}_m = \frac{-C_1 + \sqrt{C_1^2 - 4C_0 C_2}}{2C_0}$$

$$(31b) \quad \text{HE}_{mn} \text{ modes : } \mathcal{J}_m = \frac{-C_1 - \sqrt{C_1^2 - 4C_0 C_2}}{2C_0} .$$

Two cases are examined to test the jump admittance condition. The relative sheet admittances are complex:

$$(32) \quad \eta_i = g_i + j b_i \begin{cases} g_i, b_i & \text{real, with:} \\ g_i = 0 & \text{lossless sheets,} \\ g_i = b_i = 0 & \text{no sheet present,} \\ 1/b_i = 0 & \text{perfectly conducting sheet.} \end{cases}$$

Substituting the condition for no sheet, $\eta_i = 0$, (30) obviously reduces to the equation for the step-index guide [1],

$$(33) \quad \epsilon_r \mu_r \mathcal{J}_m^2 + \mathcal{J}_m \mathcal{K}_m (\epsilon_r + \mu_r) - (mb_0)^2 \left(\frac{1}{u^2} + \frac{1}{q^2} \right)^2 = 0 .$$

Next, the metallic boundary of a perfect conductor is a particular case of an isotropic surface admittance ($\eta_3 = 0$) in the limit as $\eta_1 = \eta_2 \rightarrow \infty$. If (30) is multiplied by the factor $\frac{\mathcal{J}_m^2(u)}{\eta_1 \eta_2}$, the defining equation for the circular, metallic guide results:

$$(34) \quad \mathcal{J}_m'(u) \mathcal{J}_m(u) = 0 .$$

At the limiting cases of no sheet and a perfectly conducting sheet, the derived dispersion relation matches the dispersion relations for the step-index fiber and the circular metallic guide.

2.4 Derivation of Cutoff Conditions

2.4.1 Limits at Cutoff

To find the cutoff conditions of the various modes, (30) is examined in the limit as

$$(35a) \quad q \rightarrow 0$$

$$(35b) \quad b \rightarrow 1$$

$$(35c) \quad u \rightarrow a_0 \sqrt{\epsilon_r \mu_r - 1} \quad .$$

Under these conditions, κ_m takes the following form [4]:

$$(36a) \quad m = 0; \quad \kappa_0 \rightarrow \frac{1}{q^2 \ln \frac{1}{2}}$$

$$(36b) \quad m = 1; \quad \kappa_1 \rightarrow -\frac{1}{q^2} + \frac{1}{2} \ln \frac{q}{2}$$

$$(36c) \quad m > 1; \quad \kappa_m \rightarrow -\frac{m}{q^2} - \frac{1}{2(m-1)}.$$

A detailed derivation of the cutoff conditions is presented in Appendix B.

2.4.2 Case I. : $m > 1$ At first glance, the dispersion relation would appear to be a function of $\frac{1}{q^2}$ given the order of (36c). Upon combining the higher order terms and using the relation $q^2 = a_0^2(b_0^2 - 1)$, it is seen that $\frac{1}{q^2}$ is the highest factor. Equation (30) is multiplied by the factor $\frac{q^2}{m}$ with the following result:

$$(37) \quad \begin{aligned} & \mathcal{J}_m^2 j \eta_1 \epsilon_r \mu_r a_0 + \\ & \mathcal{J}_m \left[j \eta_1 \mu_r \left(\frac{m}{a_0} - \frac{a_0}{m-1} \right) - 2j \eta_3 \mu_r - \mu_r (1 + \eta_1 \eta_2 - \eta_3^2) - \epsilon_r \right] \\ & - \frac{1}{a_0} \left(\frac{m}{a_0} - \frac{a_0}{m-1} \right) - \frac{2m}{u^2} - \frac{j}{a_0} \left(\left(\frac{ma_0}{u^2} \right)^2 \eta_1 + 2 \frac{ma_0}{u^2} \eta_3 + \eta_2 \right) = 0 \quad . \end{aligned}$$

A numerical solution is computed from an equation of this form. The cutoff conditions are defined for modes in (31) with $m > 1$.

2.4.3 Case II. : $m = 1$ The $m = 1$ cutoff conditions are found using κ_1 as defined by (36b). After performing a similar simplifying combination as in Section 2.4.2, the dispersion relation is multiplied by $J_m(u) \frac{q^2}{i n^2}$. The result is

$$(38) \quad J_1(u)[-j\eta_1\mu_r a_0 J_1'(u) + J_1(u)] = 0 \quad ,$$

which implies the cutoff conditions:

$$(39a) \quad \text{EH}_{1n} \text{ modes : } J_1(u) = 0 \quad a_0 \neq 0$$

$$(39b) \quad \text{HE}_{1n} \text{ modes : } \frac{J_1'(u)}{u J_1(u)} = \frac{1}{j\eta_1\mu_r a_0} \quad .$$

2.4.4 Case III. : $m = 0$ For modes of the order $m = 0$, the dispersion relation factors easily. The resulting cutoff conditions from Appendix B are:

$$(40a) \quad \text{TM}_{0n} \text{ modes : } J_0(u) = 0$$

$$(40b) \quad \text{TE}_{0n} \text{ modes : } \frac{J_0'(u)}{u J_0(u)} = \frac{\epsilon_r - \eta_3^2}{j\eta_1 a_0 \epsilon_r \mu_r} \quad .$$

Since the cutoff conditions (37), (39), and (40) are a special case of the dispersion relation, it is not surprising that they also produce the expected cutoff equations when examined for the limiting cases of no sheet and a perfectly conducting sheet. Note that the EH and HE modes of the step-index fiber become respectively the corresponding order TM and TE modes of the metallic guide [10]. For $m \leq 1$, the TM and EH mode cutoff remains unchanged regardless of the lossless sheet parameters. The equation determining the cutoff frequencies becomes more complicated for higher order modes.

Given that the normalized propagation constant of (35) is real, the cutoff conditions are defined for propagating modes which are lossless. Therefore, sheet parameters contained in the preceding cutoff equations are taken as pure imaginary. Simple solutions for lossy sheets are difficult to obtain. However, such solutions are easily computed due to the availability of subroutines which calculate Bessel functions of complex arguments.

1
2
3
4
5
6
7
8
9
10
11
12
13
14
15
16
17
18
19
20
21
22
23
24
25
26
27
28
29
30
31
32
33
34
35
36
37
38
39
40
41
42
43
44
45
46
47
48
49
50
51
52
53
54
55
56
57
58
59
60
61
62
63
64
65
66
67
68
69
70
71
72
73
74
75
76
77
78
79
80
81
82
83
84
85
86
87
88
89
90
91
92
93
94
95
96
97
98
99
100

3. NUMERICAL RESULTS AND CONCLUSION

3.1 Lossless Sheet Parameters

Due to the complexity of the dispersion relation, a numerical solution is attempted. Appendix A outlines the solution and provides the FORTRAN program constructed for the purpose of obtaining the zeros of the dispersion relation. Lossless examples are examined first; the sheet admittance values are chosen to be pure imaginary. Marcuse [2] examines a step-index guide with $\epsilon_r = 1.0201$ and $\mu_r = 1.0$, plotting normalized propagation constant against normalized radius. The results of Figure 3 agree with those shown in [2]. The HE_{11} mode is actually cutoff at zero, but the curve is nearly parallel to the a_0 axis at $a_0 = 5$. The HE_{21} mode is also plotted and it is not discernible from the TE_{01} and TM_{01} curve.

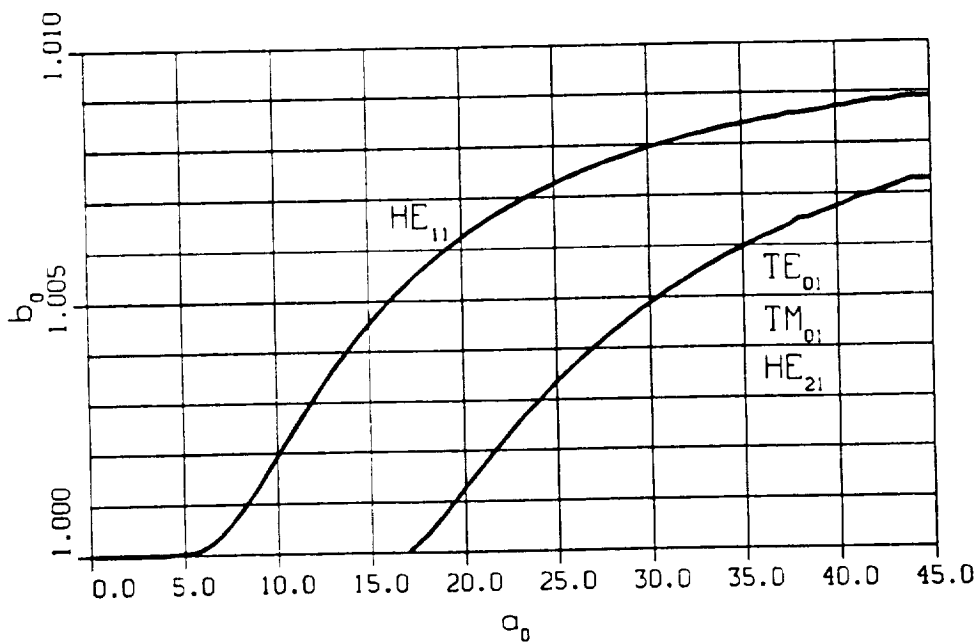


Figure 3. Normalized propagation constant vs. normalized radius for step-index fiber.

In Figure 4, plots of the step-index guide are provided with those of the corresponding modes of the circular, metallic guide. Here, the horizontal axis has been changed to the cutoff number $V = a_0 \sqrt{\epsilon_r \mu_r - 1}$. Remember, the TM_{01} cutoff value remains unchanged. In general, as η_{0i} varies from $-j0$ to $-j\infty$ (no sheet to a perfectly conducting sheet), the cutoff numbers will vary between the two curves shown. This variation is summarized in Table I., the cutoff values are computed for some of the lower order modes. As the lossless sheet values are decreased from zero, the step-index cutoff values increase towards the cutoff values of the circular, metallic guide.

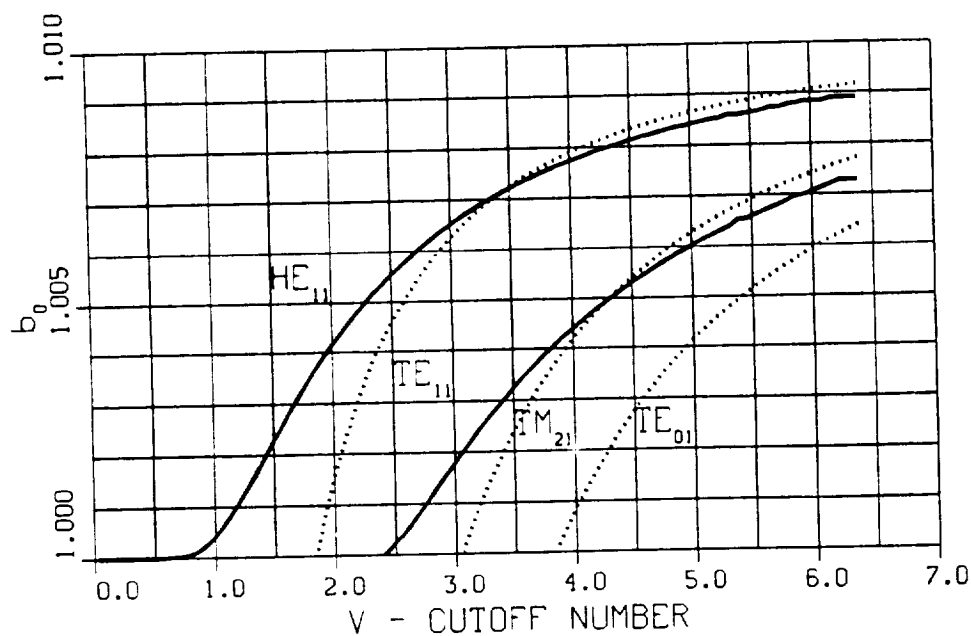


Figure 4. Normalized propagation constant vs. cutoff number, step-index fiber ——— and circular, metallic guide ······.



TABLE I. CUTOFF VALUES FOR LOSSLESS SHEETS $u = V$ At Cutoff			
$\eta_{01}, \eta_{02}, \alpha$	HE ₁₁	HE ₂₁	TE ₀₁
-j0. , -j0. , 0	0	2.41	2.41
-j.2 , -j.1 , 60	.75	2.58	3.06
-j.2 , -j.1 , 45	.86	2.71	3.14
-j.2 , -j.1 , 0	1.02	2.84	3.26
-j.3 , -j.2 , 0	1.24	2.95	3.41
-j2 , -j1 , 0	1.74	3.05	3.76
-j ∞ , -j ∞ , 0	1.84	3.05	3.83

3.2 Lossy Sheet Parameters

Suppose the sheet admittances are real or complex. Because loss terms are now present, the propagation constant will no longer be real. Instead,

$$(41) \quad b_0 = b_{0r} + j b_{0i}.$$

The field equations will contain the term

$$(42) \quad e^{b_{0i}z} e^{-j b_{0r}z},$$

where b_{0i} is the normalized attenuation constant. Therefore, solutions with $b_{0i} < 0$ will describe attenuated, propagating modes.

The remaining graphs are plots of both the real and imaginary parts of the normalized propagation constant versus normalized radius. The normalized attenuation constants have been plotted up to the cutoff values of the propagation constant. Figure 5 represents the propagation curves for the TM₀₁ mode for sheet admittances that are real. The solid curve is the step-index fiber plot. Although the cutoff radius remained unchanged in the lossless examples, it has been increased for sheet parameters with small losses. For larger losses, the TM₀₁ mode cutoff radius again becomes that of the step-index fiber.

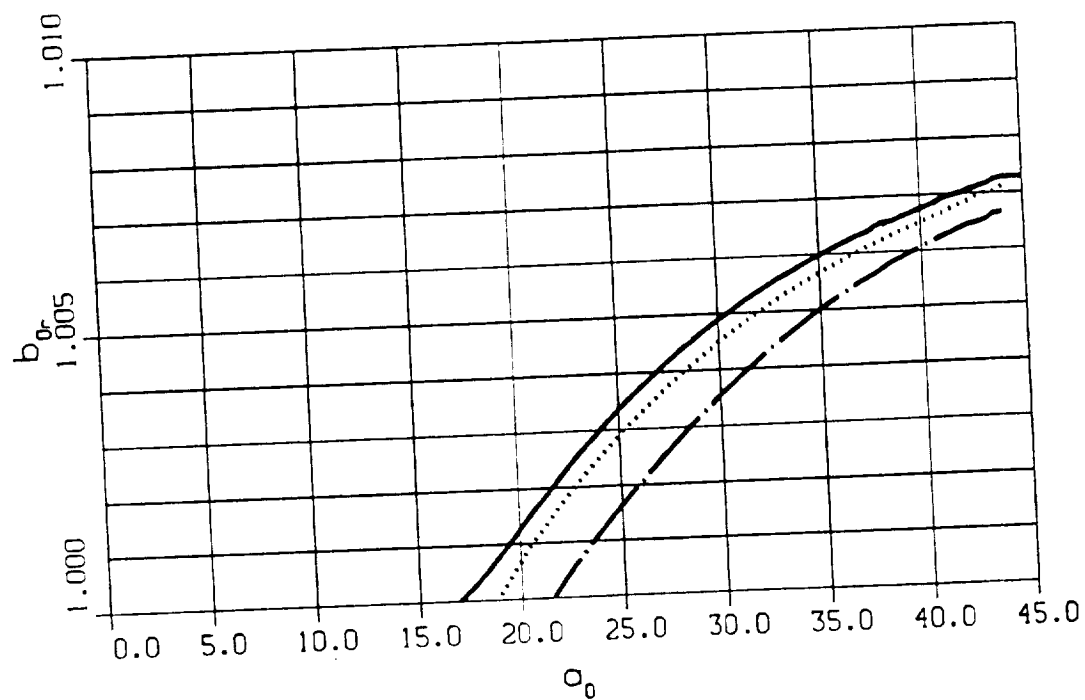


Figure 5. Normalized propagation constant versus normalized radius for TM_{01} mode with real sheet admittances.

η_{01}	η_{02}	α	
0	0	0	—
.1	.1	0
.2	.2	0	— · —
1	1	0	— — —

The corresponding attenuation curves in Figure 6 reveal that a large attenuation near cutoff occurs for $\eta_{01} = -j.2$ and becomes negligible near cutoff for $\eta_{01} = -j1$. The propagation constant curve for the $\eta_{01} = -j1$ case is not distinguishable from that of the step-index fiber.

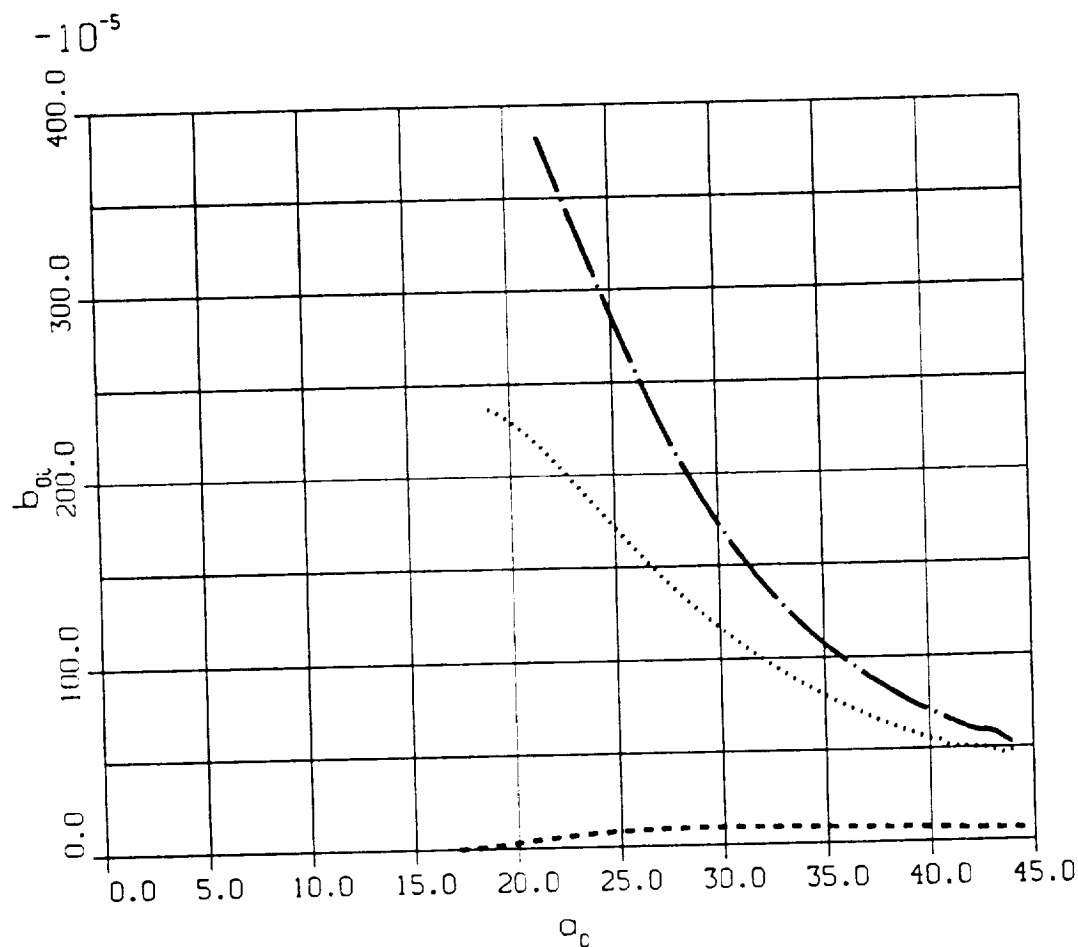


Figure 6. Normalized attenuation constant versus normalized radius for TM_{01} mode with real sheet admittances.

η_{01}	η_{02}	α	
.1	.1	0
.2	.2	0
1	1	0	-----

The same TM_{01} mode was examined for complex sheet parameters. While the propagation curves of Figure 7 are now nearly coincident, the attenuation near cutoff has been reduced significantly (Figure 8).

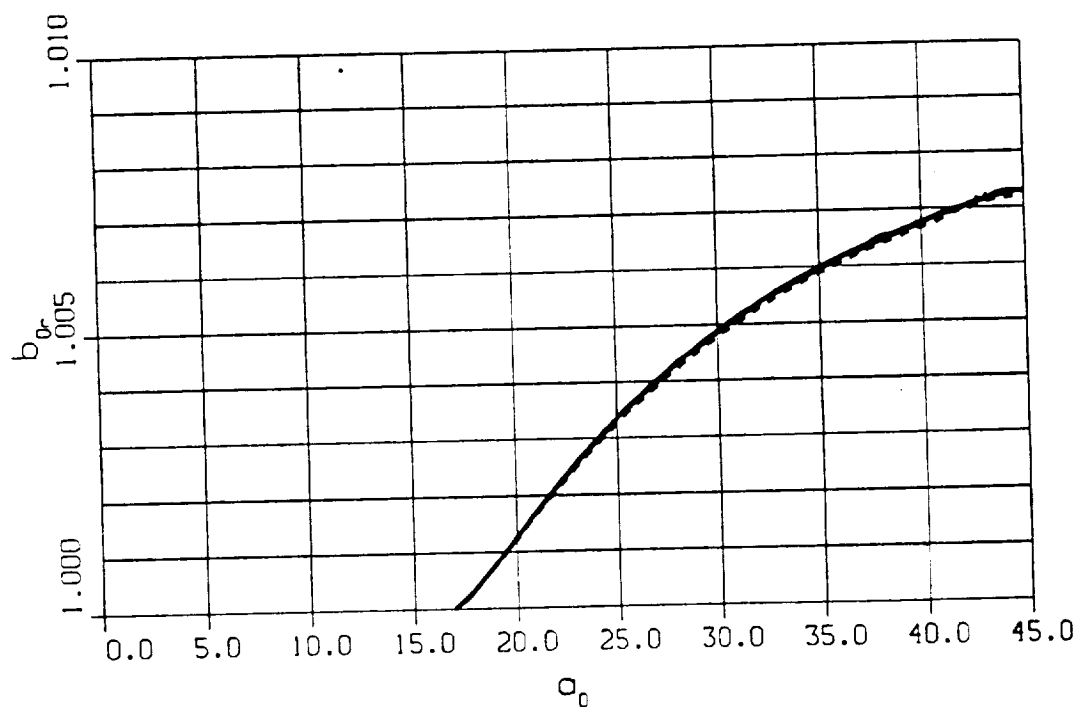


Figure 7. Normalized propagation constant versus normalized radius for TM_{01} mode with complex sheet admittances.

η_{01}	η_{02}	α	
0	0	0	————
.1-j.2	.1-j.1	0
.2-j.3	.2-j.2	0	———
1-j2	1-j1	0	----

(all four curves are nearly coincident)

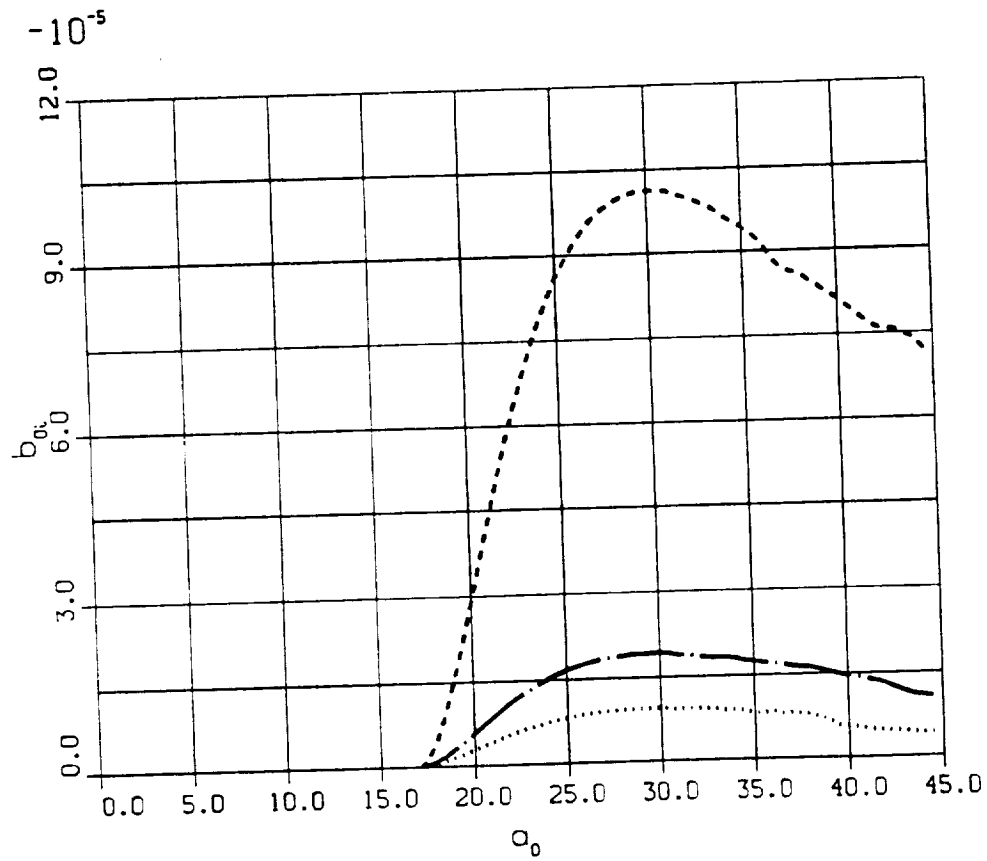


Figure 8. Normalized attenuation constant versus normalized radius for TM_{01} mode with complex sheet admittances.

η_{01}	η_{02}	α	
.1-j.2	.1-j.1	0
.2-j.3	.2-j.2	0
1-j2	1-j1	0	-----



The effect of real sheet admittances on the HE_{11} mode is now examined. Figure 9 shows the expected rise in cutoff radius.

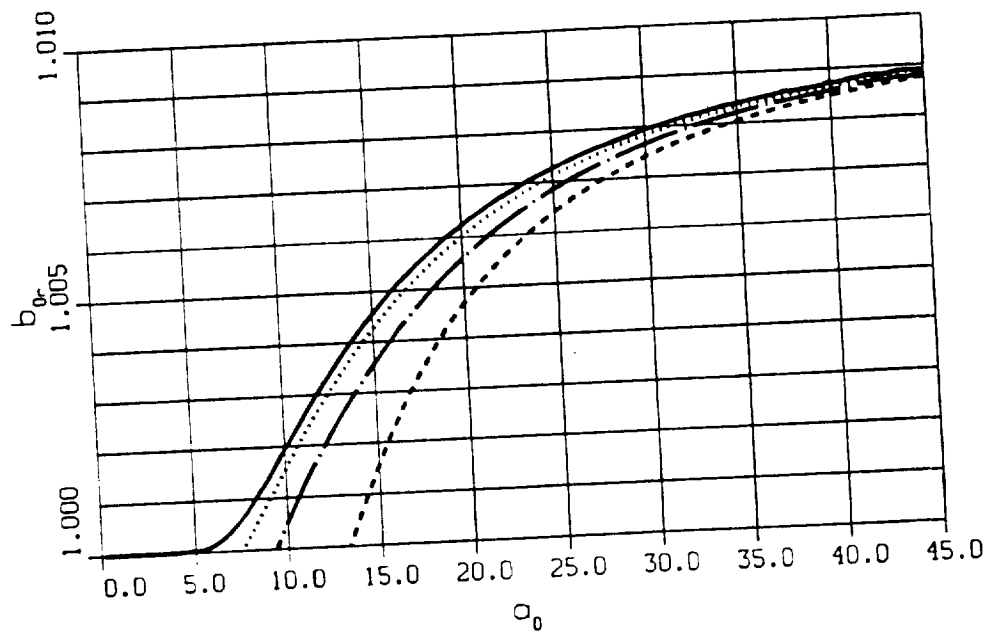
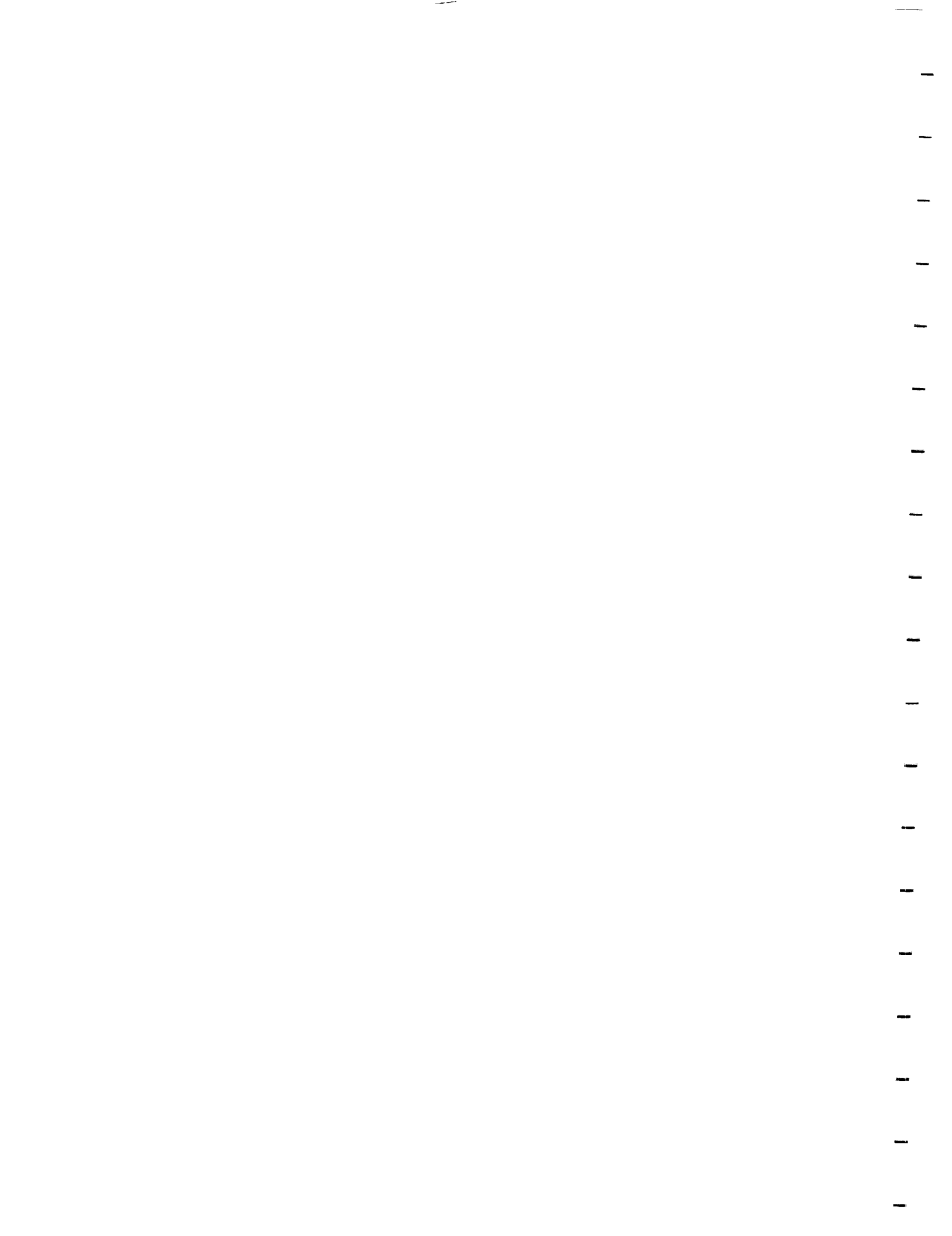


Figure 9. Normalized propagation constant versus normalized radius for HE_{11} mode with real sheet admittances.

η_{01}	η_{02}	α	
0	0	0	————
.1	.1	0
.2	.2	0	————
1	1	0	-----



Note the slight change in scale of the attenuation curve of Figure 10. The lower values of η_{01} show less attenuation near cutoff than the TM_{01} mode. However, for the $\eta_{01} = -j1$, the HE_{11} mode has the greater attenuation.

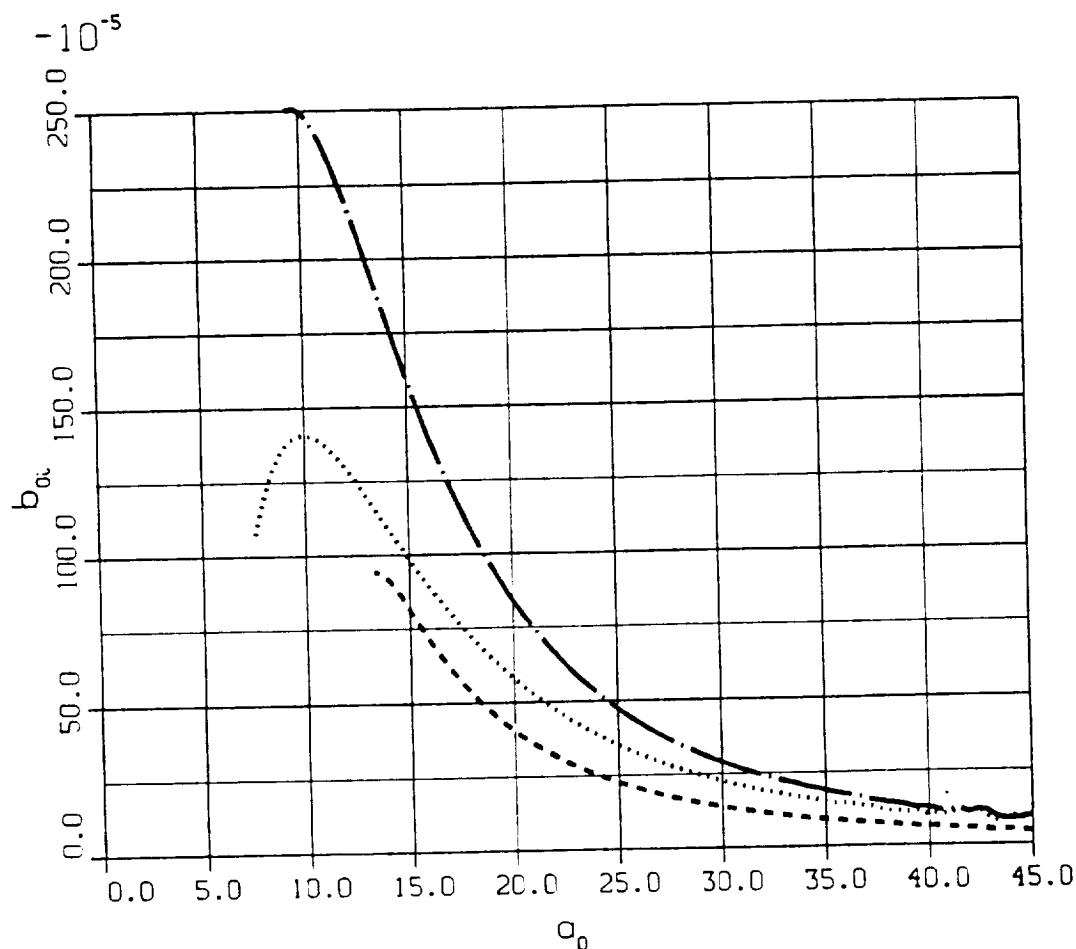


Figure 10. Normalized attenuation constant versus normalized radius for HE_{11} mode with real sheet admittances.

η_{01}	η_{02}	α	
.1	.1	0
.2	.2	0	————
1	1	0	-----

Figure 11 shows again how the complex sheet parameters tend to move the propagation curves towards the metallic guide limit.

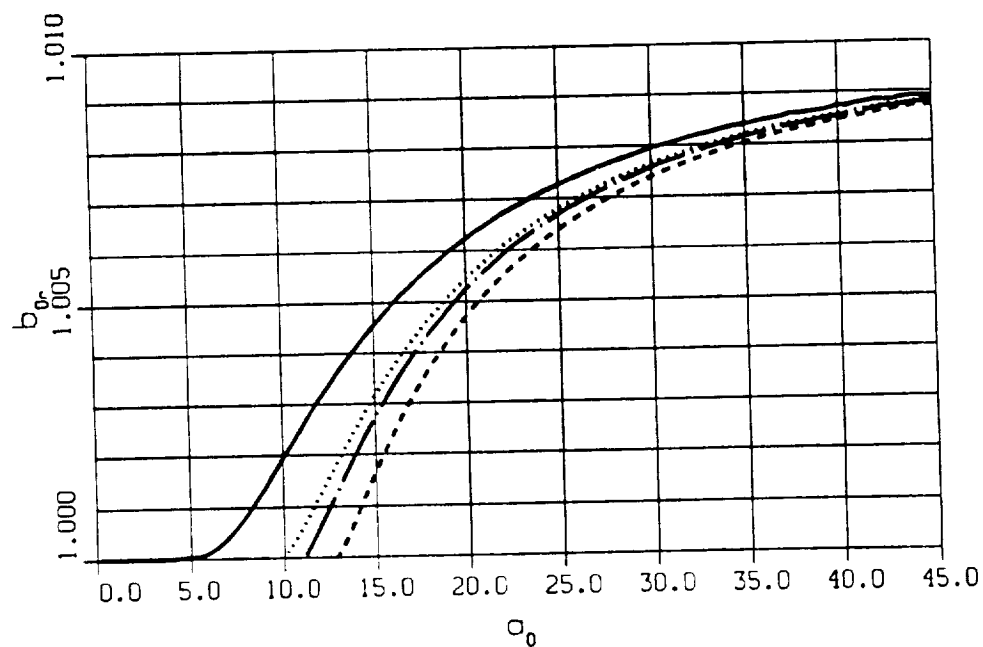


Figure 11. Normalized propagation constant versus normalized radius for HE_{11} mode with complex sheet admittances.

η_{01}	η_{02}	α	
0	0	0	————
.1-j.2	.1-j.1	0
.2-j.3	.2-j.2	0	— · — ·
1-j2	1-j1	0	----

1

2

3

4

5

6

7

8

9

10

11

12

13

14

15

16

17

18

19

20

Figure 12 shows that the complex admittances also reduce the attenuation of the HE_{11} mode, but not as large a reduction as that which resulted for the TM_{01} mode.

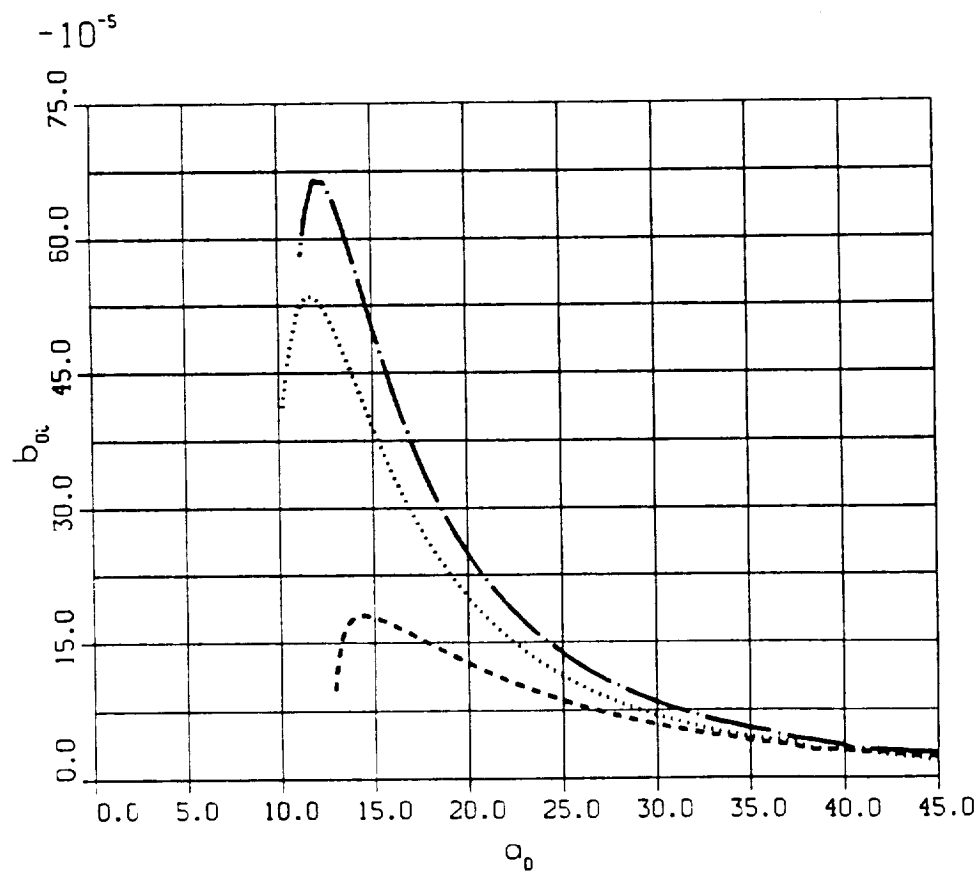


Figure 12. Normalized attenuation constant versus normalized radius for HE_{11} mode with complex sheet admittances.

η_{01}	η_{02}	α	
.1-j.2	.1-j.1	0
.2-j.3	.2-j.2	0	————
1-j2	1-j1	0	-----

Finally, Figures 13 and 14 reveal the dependence of the propagation propagation and attenuation curves on the sheet orientation. For the HE_{11} mode, increasing the parameter α has little effect on the cutoff radius, while slightly increasing the attenuation near cutoff.

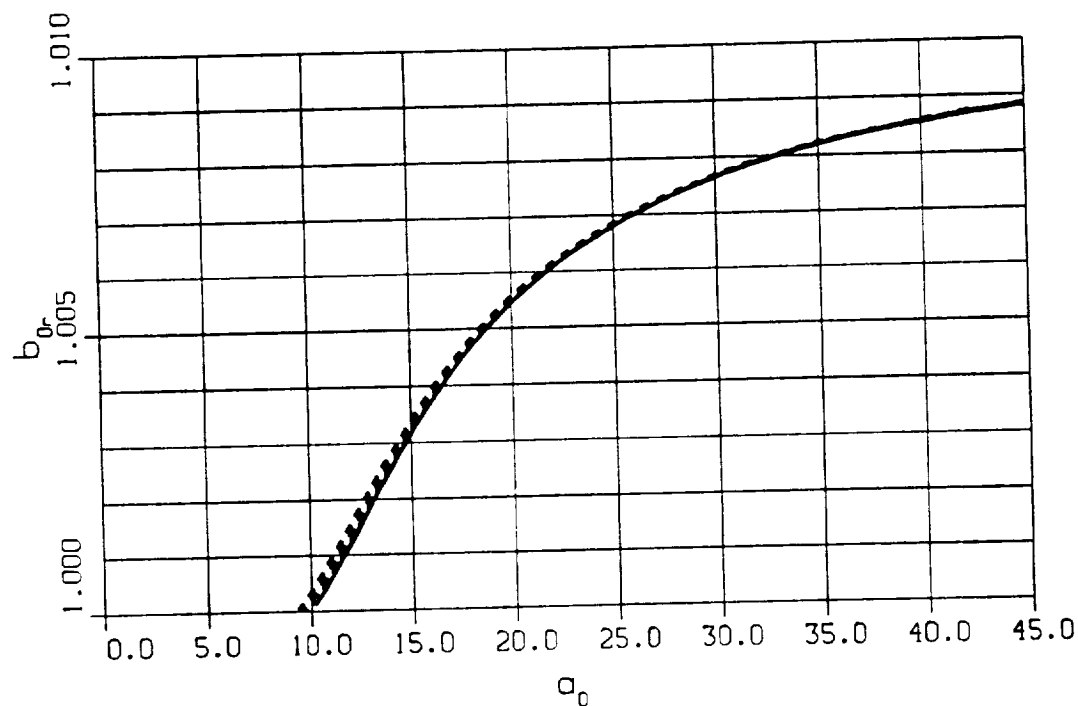
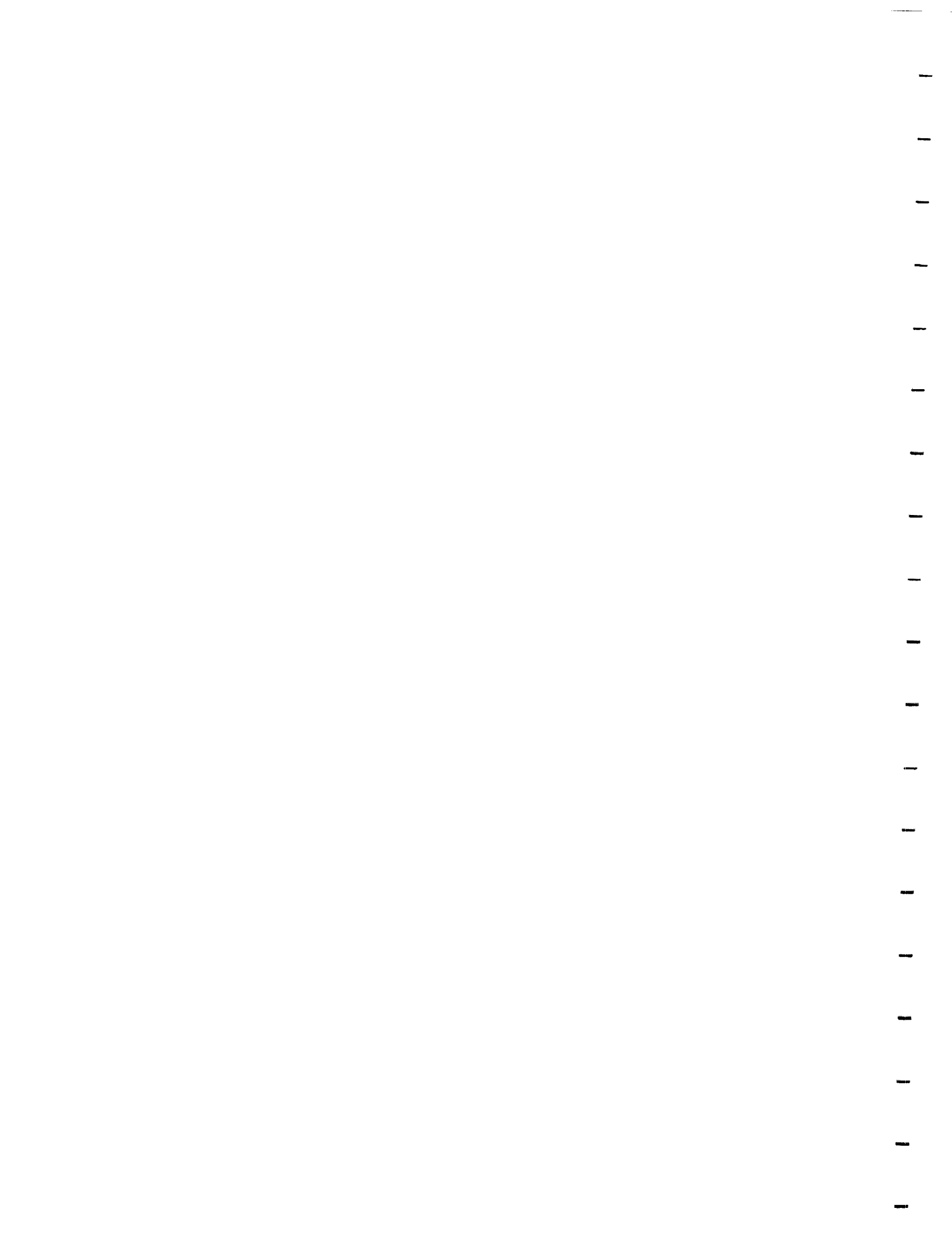


Figure 13. Normalized propagation constant versus normalized radius for HE_{11} mode with complex sheet admittances and variation in the parameter α .

η_{01}	η_{02}	α	
.1-j.2	.1-j.1	0	—
.1-j.2	.1-j.1	30
.1-j.2	.1-j.1	45	----
.1-j.2	.1-j.1	60

(all four curves nearly coincident)



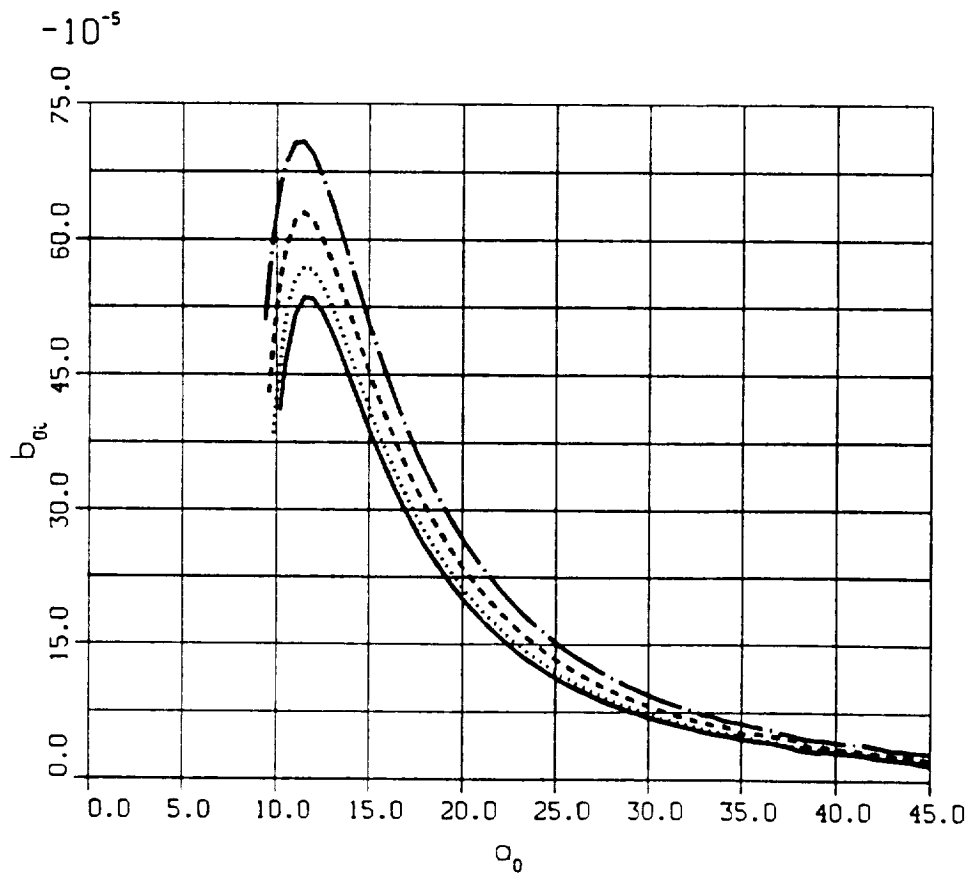
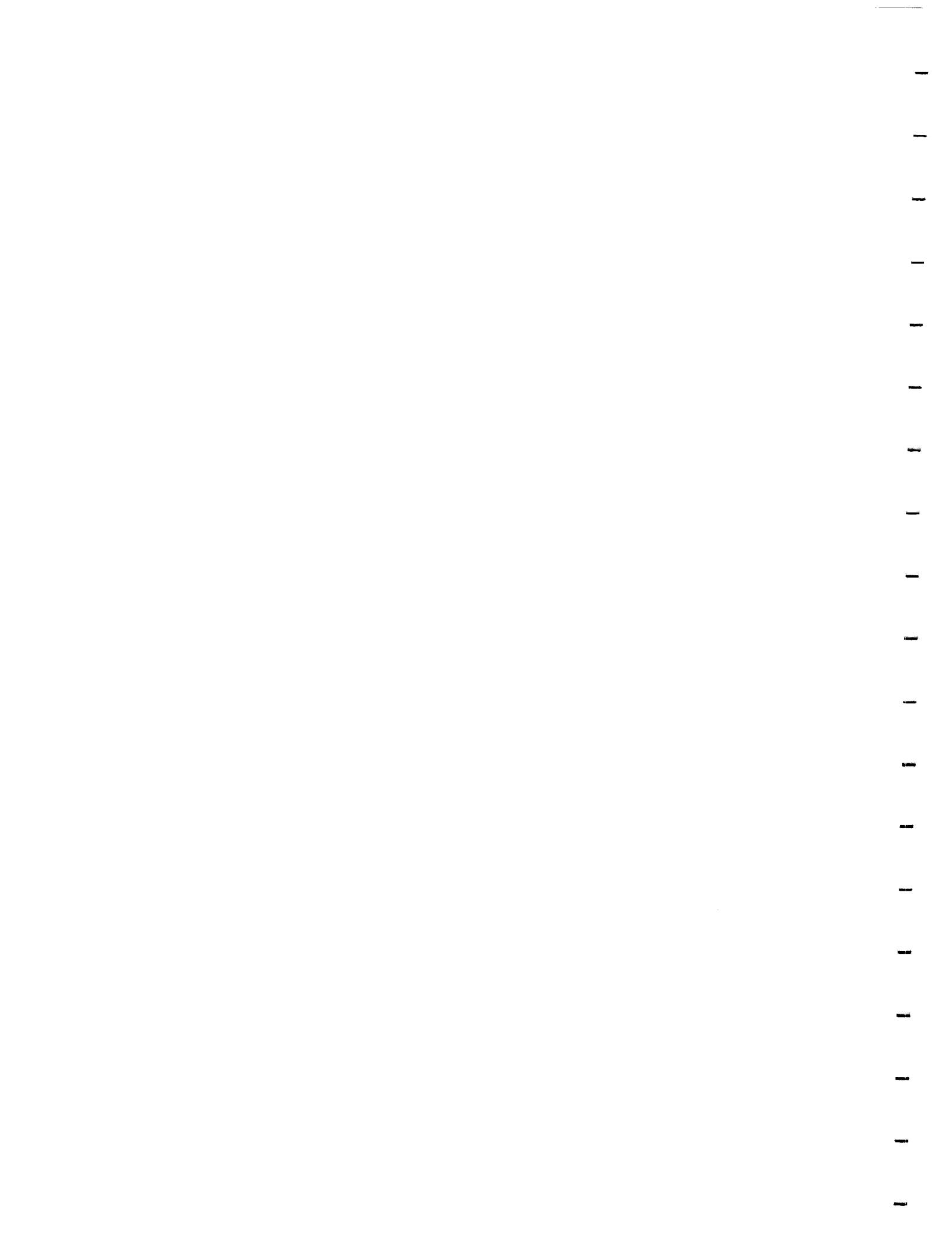


Figure 14. Normalized attenuation constant versus normalized radius for HE_{11} mode with complex sheet admittances and variation in the parameter α .

η_{01}	η_{02}	α	
.1-j.2	.1-j.1	0	—
.1-j.2	.1-j.1	30
.1-j.2	.1-j.1	45	- - -
.1-j.2	.1-j.1	60	- . - .



The general effect of the anisotropic sheet admittance is to raise the cutoff frequencies of the propagating modes. The cutoff frequencies vary from those of the step-index fiber to those of the circular, metallic guide as the sheet admittance varies from zero to infinity. Use of lossy sheets also affected the cutoff of the lower order TM modes which were unchanged in the lossless case. Attenuated, propagating modes exist when lossy sheet admittances are present, although it was shown that the attenuation could be controlled by adjusting the sheet parameters and orientation.

The dielectric waveguide analyzed is a relatively simple structure. However, the method of analysis used is easily extended to multilayered structures. Additional boundary conditions will result, the jump immittance condition is applied at each sheet interface. The method of solution will remain the same; solutions must be found for a complex valued dispersion relation.

APPENDICES

APPENDIX A. DISPERSION RELATION ROOT COMPUTATION

As stated previously, the dispersion relation, (30), is quadratic in \mathcal{J}_m . It is of the form

$$(A1) \quad C_0 \mathcal{J}_m^2 + C_1 \mathcal{J}_m + C_2 = 0$$

with,

$$(A2a) \quad C_0 = \epsilon_r \mu_r (1 - j\eta_1 a_0 \mathcal{K}_m)$$

$$(A2b) \quad C_1 = \left\{ -j\eta_1 \mu_r a_0 \mathcal{K}_m^2 + \mathcal{K}_m [\mu_r (1 + \eta_1 \eta_2 - \eta_3^2) + \epsilon_r] \right. \\ \left. + \frac{j\mu_r}{a_0} \left[\left(\frac{mb_0 a_0}{q^2} \right)^2 \eta_1 - 2 \frac{mb_0 a_0}{q^2} \eta_3 + \eta_2 \right] \right\}$$

$$(A2c) \quad C_2 = \mathcal{K}_m^2 + \frac{j\mathcal{K}_m}{a_0} \left[\left(\frac{mb_0 a_0}{u^2} \right)^2 \eta_1 + 2 \frac{mb_0 a_0}{u^2} \eta_3 + \eta_2 \right] - (mb_0)^2 \left(\frac{1}{u^2} + \frac{1}{q^2} \right)^2 = 0 .$$

By applying the quadratic formula, solutions for H-type and E-type modes are easily separated [3]:

$$(A3) \quad F(a_0, b_0) = 2C_0 \mathcal{J}_m + C_1 \pm \sqrt{C_1^2 - 4C_0 C_2} = 0.$$

The HE modes are the solutions taken from the positive radical and the EH modes are taken from the negative sign [4]. The method of solution is the Newton-Raphson technique; it is capable of determining complex roots [13] and thus accommodates both the lossless and lossy cases. The dispersion relation shown in (A3) is a function of two variables. The following FORTRAN program solves this dispersion relation for selected parameters of the dielectric core and sheet admittances ($\epsilon_r, \mu_r, \eta_{01}, \eta_{02}$, and α). Initial guesses for the Newton-Raphson technique are provided from a knowledge of the cutoff conditions or from published data for the step-index fiber [2]. The calculated root is then used as the next guess. As one of the variables is incremented, this is continued to generate

APPENDIX A. (Continued)

the dispersion and attenuation plots over the desired range. Cutoff values are obtained in a similar fashion, the cutoff equations are substituted in the function subroutine section of the program.

```

*****
C      PROGRAM DISP
C
C      THIS PROGRAM CALCULATES THE ZEROS OF THE DISPERSION RELATION FOR A
C      CYLINDRICAL WAVEGUIDE CONSISTING OF A DIELECTRIC CORE SURROUNDED
C      BY AN ANISOTROPIC SHEET IN FREE SPACE.
C
C      VARIABLE ASSIGNMENTS
C      BO - NORMALIZED PROPAGATION CONSTANT
C      KTO - NORMALIZED TRANSVERSE WAVE NUMBER INSIDE CORE
C      GTO - NORMALIZED TRANSVERSE WAVE NUMBER OUTSIDE CORE
C      AO - NORMALIZED RADIUS
C      U = KTO*AO, BESSEL ARGUMENT
C      Q = GTO*AO, MODIFIED BESSEL ARGUMENT
C      BGES - INITIAL GUESS FOR BO
C      AGES - INITIAL GUESS FOR AO
C      FOUT - VALUE OF DISPERSION RELATION
C
C      MSTART,MSTOP- RANGE OF BESSEL ORDER
C      HSTART,HSTOP- RANGE OF MODE TYPE (HE=0, EH=1)
C
C      EPSR - CORE RELATIVE PERMITTIVITY
C      MUR - CORE RELATIVE PERMEABILITY
C
C      NO1,NO2,ANG- SHEET PARAMETERS
C      N1,N2,N3 - TRANSFORMED SHEET PARAMETERS
C
*****
C-----
C      COMMON BLOCK PARAM PASSES BACK MEDIA DATA AND TRANSVERSE WAVE NOS.
C      BETWEEN SUBROUTINES.
C
C      COMMON /PARAM/ U,KTO,Q,GTO,NO1,NO2,ANG,EPSR,MUR,ITS2,NIN2
C      COMPLEX U,KTO,Q,GTO,NO1,NO2
C      REAL ANG,EPSR,MUR,R
C      INTEGER ITS2,NIN2
C-----
C      INTEGER MSTART,MSTOP,M,HSTART,HSTOP,H,ITS,INC2,AMIN
C      REAL AO,AGES,REF,DEC
C      COMPLEX BO,BGES,FOUT,F
C      EXTERNAL NEWT,CBJNS
C
C      3  FORMAT (1X,I2)
C-----
C      READ IN DATA AND INIT GUESS
C
C      OPEN(UNIT=79,STATUS='OLD')
C
C      READ(79,7)EPSR,MUR
C      7  FORMAT(1X,2(F8.4,2X))
C
C      READ(79,9)NO1,NO2,ANG
C      9  FORMAT(1X,5(F8.4,2X))
C
C      READ(79,11)AMIN,MSTART,MSTOP,HSTART,HSTOP
C      11  FORMAT(1X,5(14,2X))
C
C      READ(79,13)BGES,AGES,ITS
C      13  FORMAT(1X,3(F10.5,2X),I3)

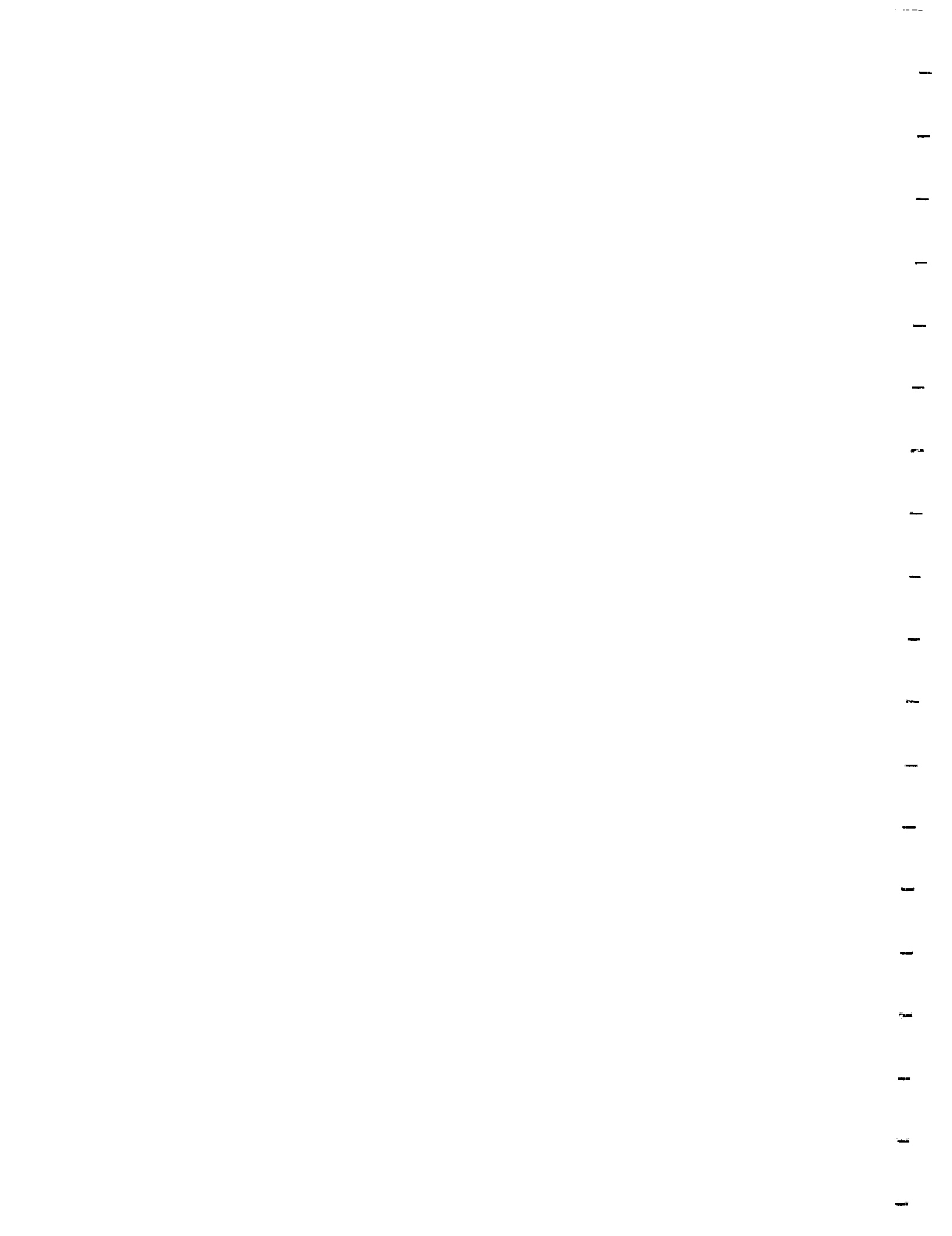
```

DIELECTRIC PARAMETERS

SHEET PARAMETERS

MIN RADIUS, MODE ORDER/TYPE

INIT. VALUES AND ITERATIONS



APPENDIX A. (Continued)

```

CLOSE(UNIT=79)

C
C OPEN OUTPUT FILE
C
OPEN(UNIT=80)
WRITE(80,*)(' EPSR           MUR')
WRITE(80,7)EPSR,MUR
WRITE(80,*)(' NO1           NO2           ANG')
WRITE(80,9)NO1,NO2,ANG
WRITE(80,*)(' MIN RAD      MSTART  MSTOP  HSTART  HSTOP')
WRITE(80,11)AMIN,MSTART,MSTOP,HSTART,HSTOP
WRITE(80,*)(' BO GUESS      AO GUESS      ITERATIONS')
WRITE(80,13)BGES,AGES,ITS

C-----
C*****
C CALCULATE ZEROS OF DISPERSION RELATION
C*****
WRITE(6,*)('DO YOU WANT ITERATIONS PRINTED?')
WRITE(6,*)('REAL ROOTS: Y(1) N(2)   COMPLEX:Y(-1),N(-2)')
READ(6,3)NIN2
WRITE(6,*)('INPUT RADIUS INCREMENT?')
WRITE(6,*)('DEC=IDEC*.1')
READ(6,3)IDEC
REF=SQRT(EPSR*MUR)

C
WRITE(80,*)(' MODE TYPE')
WRITE(80,*)('H='),H
DO 1 H=HSTART,HSTOP
DO 2 M=MSTART,MSTOP
BO=BGES
AO=AGES
R=FLOAT(AMIN)
DEC=FLOAT(IDEC)*.1
ITS2=ITS
WRITE(80,*)(' ROOT FILE')
WRITE(80,*)('M='),M
WRITE(80,*)(' AO      BO      U      Q      FOUT')
WRITE(80,39)
39  FORMAT (3(/))

C DO LOOP SEARCHES FOR ROOTS WITHIN THE BOUNDS OF BO FOR
C PROPAGATING MODES
C
DO 4 WHILE ((REAL(BO) .GE. 1.)
& .AND. (REAL(BO) .LE. REF)
& .AND. (AO .GT. R))
CALL NEWT(BO,AO,M,H,FOUT)
WRITE(6,*)AO,BO,U
WRITE(80,14)AO,BO,U,FOUT
14  FORMAT(1X,2(F10.5),2X,E12.5,4(F8.4))
AO=AO-DEC
4  ENDDO
2  CONTINUE
1  CONTINUE
CLOSE(UNIT=80)
STOP
99  END

C
C*****
C COMPLEX FUNCTION F CALCULATES THE VALUE OF THE DISPERSION RELATION
C*****
C
C
C COMPLEX FUNCTION F(BO,AO,M,H)
C-----
C COMMON BLOCK PARAM PASSES BACK MEDIA DATA AND TRANSVERSE WAVE NOS.
C BETWEEN SUBROUTINES.
C

```

—

—

—

—

—

—

—

—

—

—

—

—

—

—

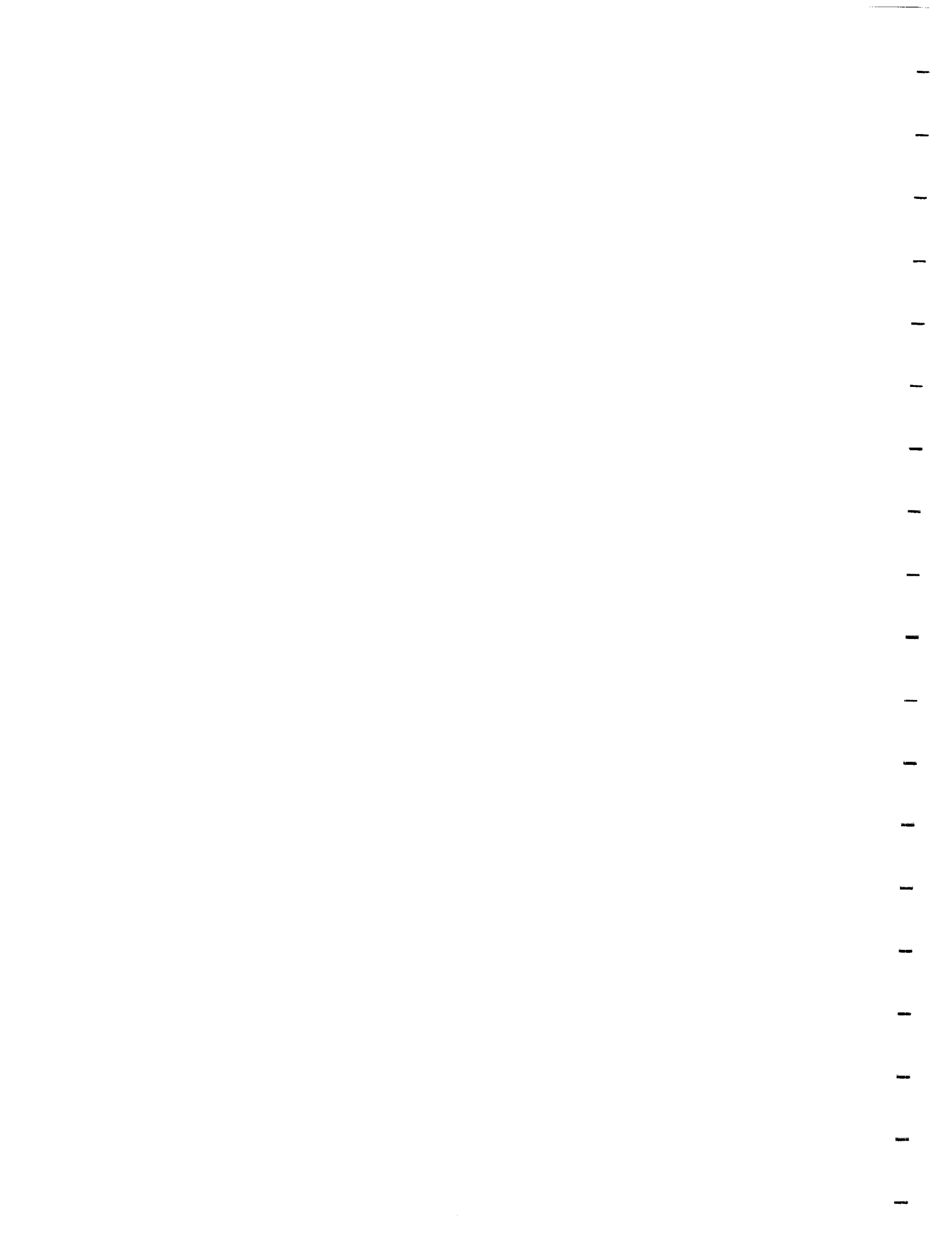
—

—

—

—

—



பாடகர்

```

SUBROUTINE NEWT VARIABLES
  FP - APPROXIMATES DERIVATIVE OF DISPERSION RELATION OVER
        THE INTERVAL INC IN B0

```

```

INTEGER M,H
REAL AO
COMPLEX BO,FOUT,F,FP,INC
INC=(.10E-06,0.)
IF (NIN2 .LT. 0) THEN
INC=INC*(1.,1.)
ENDIF
I=1
DO 12 WHILE ((REAL(BO) .GE. 1.)
& .AND. (REAL(BO) .LE. (SQRT(EPSR*MUR)))
& .AND. (I .LT. ITS2))
FP=(F(BO+INC,AO,M,H)-F(BO,AO,M,H))/INC
BO=BO-(F(BO,AO,M,H)/FP)
FOUT=F(BO,AO,M,H)
IF (ABS(NIN2) .EQ. 1) THEN
WRITE(6,21)AO,BO,U,Q,FOUT
21 FORMAT(1X,9(F8.4,2X))
ENDIF
I=I+1
12 ENDDO
RETURN
END

```


APPENDIX B. DERIVATION OF CUTOFF CONDITIONS

B.1 Limits at Cutoff

To find the cutoff conditions of the various modes, the dispersion relation

$$\begin{aligned}
 & \mathcal{J}_m^2 \epsilon_r \mu_r (1 - j \eta_1 a_0 \mathcal{K}_m) \\
 & + \mathcal{J}_m \left\{ -j \eta_1 \mu_r a_0 \mathcal{K}_m^2 + \mathcal{K}_m [\mu_r (1 + \eta_1 \eta_2 - \eta_3^2) + \epsilon_r] \right. \\
 & \quad \left. + \frac{j \mu_r}{a_0} \left[\left(\frac{mb_0 a_0}{q^2} \right)^2 \eta_1 - 2 \frac{mb_0 a_0}{q^2} \eta_3 + \eta_2 \right] \right\} \\
 (B1) \quad & + \mathcal{K}_m^2 + \frac{j \mathcal{K}_m}{a_0} \left[\left(\frac{mb_0 a_0}{u^2} \right) \eta_1 + 2 \frac{mb_0 a_0}{u^2} \eta_3 + \eta_2 \right] - (mb_0)^2 \left(\frac{1}{u^2} + \frac{1}{q^2} \right)^2 = 0 .
 \end{aligned}$$

is examined in the limit as

$$(B2a) \quad q \rightarrow 0$$

$$(B2b) \quad b \rightarrow 1$$

$$(B2c) \quad u \rightarrow a_0 \sqrt{\epsilon_r \mu_r - 1} .$$

Under these conditions, \mathcal{K}_m takes the following form [4]:

$$(B3a) \quad m = 0; \quad \mathcal{K}_0 \rightarrow \frac{1}{q^2 \ln \frac{q}{2}}$$

$$(B3b) \quad m = 1; \quad \mathcal{K}_1 \rightarrow -\frac{1}{q^2} + \frac{1}{2} \ln \frac{q}{2}$$

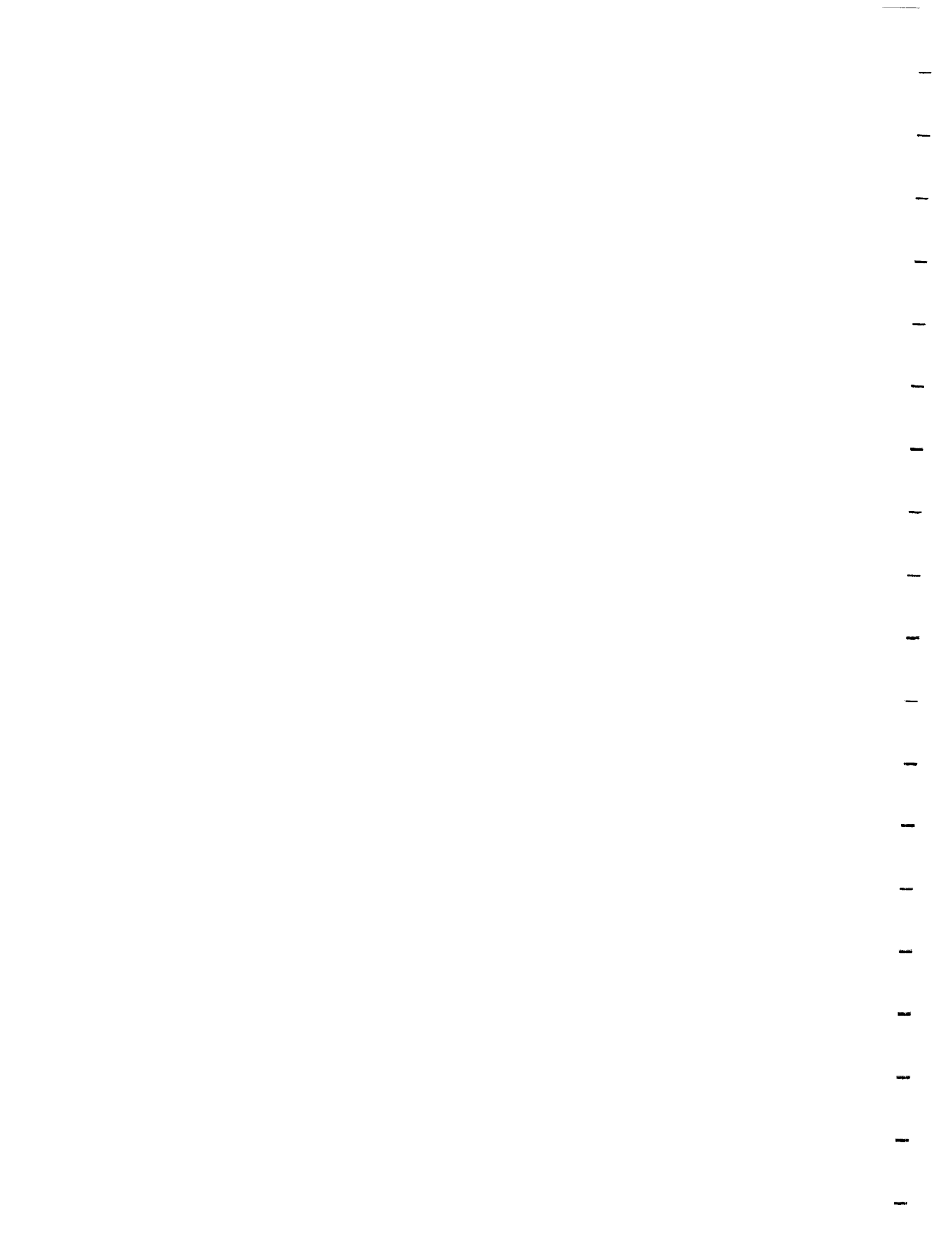
$$(B3c) \quad m > 1; \quad \mathcal{K}_m \rightarrow -\frac{m}{q^2} - \frac{1}{2(m-1)} .$$

B.2 Case I. : $m > 1$

Equation (B1) is multiplied out and the factors of q are collected. Note that

$$(B4a) \quad \left(\frac{1}{u^2} + \frac{1}{q^2} \right)^2 = \frac{1}{q^4} + \frac{2}{u^2 q^2} + \frac{1}{u^4}$$

$$(B4b) \quad \mathcal{K}_m^2 = \frac{m^2}{q^4} + \frac{m}{(m-1)q^2} + \frac{1}{4(m-1)^2} .$$



APPENDIX B. (Continued)

The dispersion relation will be of the form $X/q^2 + Y$. Therefore, constant terms with no q dependence will be dropped. They will approach zero as the equation is multiplied by q^2 and q approaches zero. The surviving terms are

$$\begin{aligned}
 & \mathcal{J}_m^2 \left(\frac{1}{q^2} \right) (j\eta_1 \epsilon_r \mu_r a_0 m) + \\
 & \mathcal{J}_m \left(\frac{1}{q^4} \right) [j\eta_1 \mu_r a_0 m^2 (b_0^2 - 1)] \\
 & \mathcal{J}_m \left(\frac{1}{q^2} \right) \left[-j\eta_1 \mu_r a_0 \frac{m}{m-1} - 2j\eta_3 \mu_r m b_0 - m(\mu_r(1 + \eta_1 \eta_2 - \eta_3^2) + \epsilon_r) \right] \\
 (B5) \quad & - \left(\frac{1}{q^4} \right) (b_0^2 - 1) - \left(\frac{1}{q^2} \right) \left[\frac{m}{m-1} - 2 \left(\frac{mb_0}{u} \right)^2 - j \frac{m}{a_0} \left[\left(\frac{mb_0 a_0}{u^2} \right)^2 \eta_1 + 2 \frac{mb_0 a_0}{u^2} \eta_3 + \eta_2 \right] \right] .
 \end{aligned}$$

Since $a_0^2(b_0^2 - 1) = q^2$, (B5) actually contains terms of highest order $\frac{1}{q^2}$,

$$\begin{aligned}
 & \mathcal{J}_m^2 \left(\frac{m}{q^2} \right) j\eta_1 \epsilon_r \mu_r a_0 \\
 & \mathcal{J}_m \left(\frac{m}{q^2} \right) \left[j\eta_1 \mu_r \left(\frac{m}{a_0} - \frac{a_0}{m-1} \right) - 2j\eta_3 \mu_r - \mu_r(1 + \eta_1 \eta_2 - \eta_3^2) - \epsilon_r \right] \\
 (B6) \quad & - \frac{m}{q^2 a_0} \left(\frac{m}{a_0} - \frac{a_0}{m-1} \right) - \frac{2m}{u^2} - \frac{j}{a_0} \left(\left(\frac{ma_0}{u^2} \right)^2 \eta_1 + 2 \frac{ma_0}{u^2} \eta_3 + \eta_2 \right) = 0 .
 \end{aligned}$$

Multiplying (B6) by q^2/m , the result is,

$$\begin{aligned}
 & \mathcal{J}_m^2 j\eta_1 \epsilon_r \mu_r a_0 \\
 & \mathcal{J}_m \left[j\eta_1 \mu_r \left(\frac{m}{a_0} - \frac{a_0}{m-1} \right) - 2j\eta_3 \mu_r - \mu_r(1 + \eta_1 \eta_2 - \eta_3^2) - \epsilon_r \right] \\
 (B7) \quad & - \frac{1}{a_0} \left(\frac{m}{a_0} - \frac{a_0}{m-1} \right) - \frac{2m}{u^2} - \frac{j}{a_0} \left(\left(\frac{ma_0}{u^2} \right)^2 \eta_1 + 2 \frac{ma_0}{u^2} \eta_3 + \eta_2 \right) = 0 ,
 \end{aligned}$$

which is equivalent to (37), the cutoff equation for the $m > 1$ modes.



APPENDIX B. (Continued)

B.3 Case II. : $m = 1$

For the $m = 1$ cutoff conditions, use κ_1 from (B3b) and

$$(B8) \quad \kappa_1^2 = \frac{1}{q^4} - \frac{\ln \frac{q}{2}}{q^2} + (\ln \frac{q}{2})^2.$$

(B1) is multiplied by $\frac{q^2}{\ln \frac{q}{2}}$, this allows removal of the terms containing $(\kappa_m)^1$, terms up to the order $\frac{1}{q^2}$, and constants with respect to q . The surviving terms are

$$(B9) \quad \left(\frac{q^2}{\ln \frac{q}{2}}\right)[-j\eta_1\mu_r a_0 \mathcal{J}_m + 1][\kappa_m^2 - m^2 b_0^2] = 0.$$

With applications of De l'Hospital's Rule, this is equivalent to

$$(B10) \quad -j\eta_1\mu_r a_0 \mathcal{J}_1 + 1 = 0.$$

Equation (B10) is the same as (39), the cutoff equation for the $m = 1$ modes.

B.4 Case III. : $m = 0$

Letting $m = 0$, the remaining terms of (B1) are,

$$(B11) \quad \begin{aligned} & \mathcal{J}_0^2 \epsilon_r \mu_r (1 - j\eta_1 a_0 \kappa_0) \\ & + \mathcal{J}_0 \left\{ -j\eta_1 \mu_r a_0 \kappa_0^2 + \kappa_0 [\mu_r (1 + \eta_1 \eta_2 - \eta_3^2) + \epsilon_r] + \frac{j\mu_r \eta_2}{a_0} \right\} \\ & + \kappa_0^2 + \frac{j\kappa_0 \eta_2}{a_0} = 0. \end{aligned}$$

This equation actually factors into the following two solutions

$$(B12a) \quad \text{TEcase} \quad \mathcal{J}_0 = \frac{\kappa_0(\epsilon_r - \eta_3^2)}{\epsilon_r \mu_r (1 - j\eta_1 a_0 \kappa_0)}$$

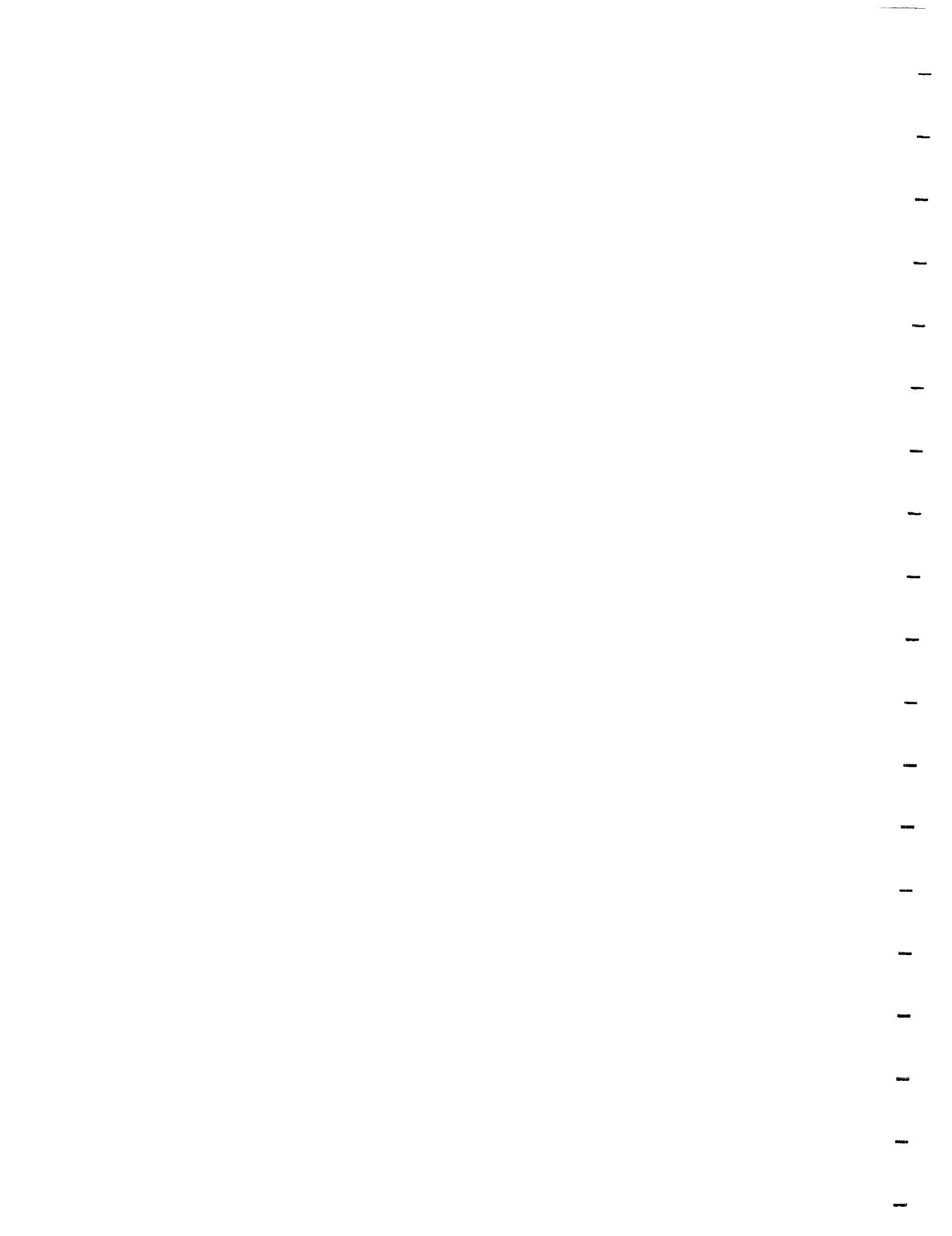
$$(B12b) \quad \text{TMcase} \quad \mathcal{J}_0 = \frac{-1}{\epsilon_r} (\kappa_0 + j \frac{\eta_2}{a_0}).$$

As κ_0 becomes large at cutoff, these reduce to the quantities in (40) by inspection,

$$(B13a) \quad \text{TM}_{0n} \text{ modes : } J_0(u) = 0$$

$$(B13b) \quad \text{TE}_{0n} \text{ modes : } \frac{J'_0(u)}{u J_0(u)} = \frac{\epsilon_r - \eta_3^2}{j\eta_1 a_0 \epsilon_r \mu_r}.$$

From equation (B12b), it is apparent cutoff frequencies of the lossless TM_{01} modes are not affected by sheet parameters.



CITED LITERATURE

1. Cherin, Allen H. : An Introduction to Optical Fibers. New York, McGraw-Hill, 1983.
2. Marcuse, Dietrich : Light Transmission Optics. New York, Van Nostrand Reinhold, 1982.
3. Yariv, Amnon : Optical Electronics . New York, Holt, Reinhart, and Winston, 1985.
4. Kapany, N. S., and Burke, J. : Optical Waveguides . Academic Press, 1972.
5. Tonning, Andreas : An Alternative Theory of Optical Waveguides with Radial Inhomogeneities. *IEEE Trans. Microwave Theory and Tech.*, MTT-30, no. 5: 781-789, 1982.
6. Tonning, Andreas : Circularly Optical Waveguide with Strong Anisotropy. *IEEE Trans. Microwave Theory and Tech.*, MTT-30, no. 5: 790-794, 1982.
7. Lindell, I. V., and Oksanen, M. I. : Transversely Anisotropic Optical Fibers: Variational Analysis of a Nonstandard Eigenproblem. *IEEE Trans. Microwave Theory and Tech.* , MTT-31, no. 9: 736-744, 1983.
8. Lindell, I. V., and Oksanen, M. I. : Complex-valued Functionals in Variational Analysis of Waveguides with Impedance Boundaries. *IEE Transactions Part H*, Vol 136, no. 4: 281-288, 1989.
9. Elsherbeni, A. Z., Stanier, J., and Hamid, M. : Eigenvalues of Propagating Waves in a Circular Waveguide with an Impedance Wall. *IEE Transactions Part H*, Vol 135, no. 4: 23-26, 1988.
10. Chou, R., and Lee, S. : Modal Attenuation in Multilayered Coated Waveguides. *IEEE Trans. Microwave Theory and Tech.*, MTT-36, no. 7: 1167-1176, 1988.
11. Graglia, R. D., and Uslenghi, P. L. E. : Anisotropic Layered Absorbers on Cylindrical Structures. *Electromagnetics*, 7: 117-127, 1987.
12. Eaves, R. E. : Electromagnetic Boundary Conditions for Laminar Regions. *Journ. Phys. D: Appl. Phys.*, Vol. 5: 2145-2151, 1972.
13. McCracken, D., and Dorn, W. : Numerical Methods and Fortran Programming . New York, Wiley, 1964.
14. Uslenghi, P. L. E. : EECS 420 Electromagnetic Field Theory Lectures . University of Illinois at Chicago, 1987.

VITA

NAME: Jerome Thomas Kish

EDUCATION: B.S., Electrical Engineering, University of Illinois,
Urbana, Illinois, 1987

M.S., Electrical Engineering, University of Illinois,
Chicago, Illinois, 1990

WORK
EXPERIENCE: Sargent and Lundy, Engineers
Consulting Engineering for Power Industry
Chicago, Illinois, 1985

Andrew Corporation
Microwave Components and Broadcast Division
Orland Park, Illinois, 1986-90

HONORS: Undergraduate James Scholar, University of Illinois,
Urbana, 1985

Eta Kappa Nu Electrical Engineering Honor Society

Professional Engineer-Fundamentals of Engineering Exam

Winner of IEEE Chicago Chapters of Antennas and Propagation-
Microwave Theory and Techniques Student Paper Contest, 1989

Member of IEEE, MTT and APS Societies

